

Deep learning-based numerical methods for high-dimensional parabolic partial differential equations and backward stochastic differential equations

Weinan E¹, Jiequn Han², and Arnulf Jentzen³

¹Beijing Institute of Big Data Research (China), Princeton University (USA), and Peking University (China), e-mail: weinan (at) math.princeton.edu

²Princeton University (USA), e-mail: jiequnh (at) princeton.edu

³ETH Zurich (Switzerland), e-mail: arnulf.jentzen (at) sam.math.ethz.ch

June 16, 2017

Abstract

We propose a new algorithm for solving parabolic partial differential equations (PDEs) and backward stochastic differential equations (BSDEs) in high dimension, by making an analogy between the BSDE and reinforcement learning with the gradient of the solution playing the role of the policy function, and the loss function given by the error between the prescribed terminal condition and the solution of the BSDE. The policy function is then approximated by a neural network, as is done in deep reinforcement learning. Numerical results using `TENSORFLOW` illustrate the efficiency and accuracy of the proposed algorithms for several 100-dimensional nonlinear PDEs from physics and finance such as the Allen-Cahn equation, the Hamilton-Jacobi-Bellman equation, and a nonlinear pricing model for financial derivatives.

Contents

1	Introduction	2
2	Main ideas of the algorithm	3
2.1	An example: a semilinear heat partial differential equation (PDE)	4
2.2	Formulation of the PDE as a suitable stochastic control problem	4
2.3	The nonlinear Feynman-Kac formula	5
2.4	Forward discretization of the backward stochastic differential equation (BSDE)	5

2.5	Deep learning-based approximations	6
2.6	Stochastic optimization algorithms	6
3	Details of the algorithm	7
3.1	Formulation of the proposed algorithm in the case of semilinear heat equations	7
3.2	Formulation of the proposed algorithm in the general case	8
3.3	Comments on the proposed algorithm	9
4	Examples for nonlinear partial differential equations (PDEs) and nonlinear backward stochastic differential equations (BSDEs)	9
4.1	Setting	10
4.2	Allen-Cahn equation	12
4.3	A Hamilton-Jacobi-Bellman (HJB) equation	13
4.4	Pricing of European financial derivatives with different interest rates for borrowing and lending	18
4.5	Multidimensional Burgers-type PDEs with explicit solutions	20
4.6	An example PDE with quadratically growing derivatives and an explicit solution	24
4.7	Time-dependent reaction-diffusion-type example PDEs with oscillating explicit solutions	24
5	Appendix A: Special cases of the proposed algorithm	27
5.1	Stochastic gradient descent (SGD)	27
5.2	Adaptive Moment Estimation (Adam) with mini-batches	27
5.3	Geometric Brownian motion	28
5.4	Euler-Maruyama scheme	29
6	Appendix B: PYTHON and MATLAB source codes	29
6.1	PYTHON source code for an implementation of the deep BSDE solver in the case of the Allen-Cahn PDE (35) in Subsection 4.2	29
6.2	MATLAB source code for the Branching diffusion method used in Subsection 4.2	34
6.3	MATLAB source code for the classical Monte Carlo method used in Subsection 4.3	36

1 Introduction

Developing efficient numerical algorithms for high dimensional (say, hundreds of dimensions) partial differential equations (PDEs) has been one of the most challenging tasks in applied mathematics. As is well-known, the difficulty lies in the “curse of dimensionality” [1], namely, as the dimensionality grows, the complexity of the algorithms grows exponentially. For this reason, there are only a limited number of cases where practical

high dimensional algorithms have been developed. For linear parabolic PDEs, one can use the Feynman-Kac formula and Monte Carlo methods to develop efficient algorithms to evaluate solutions at any given space-time locations. For a class of inviscid Hamilton-Jacobi equations, Darbon & Osher have recently developed an algorithm which performs numerically well in the case of such high dimensional inviscid Hamilton-Jacobi equations; see [9]. Darbon & Osher’s algorithm is based on results from compressed sensing and on the Hopf formulas for the Hamilton-Jacobi equations. A general algorithm for (nonlinear) parabolic PDEs based on the Feynman-Kac and Bismut-Elworthy-Li formula and a multi-level decomposition of Picard iteration was developed in [11] and has been shown to be quite efficient on a number examples in finance and physics. The complexity of the algorithm is shown to be $O(d\varepsilon^{-4})$ for semilinear heat equations, where d is the dimensionality of the problem and ε is the required accuracy.

In recent years, a new class of techniques, called deep learning, have emerged in machine learning and have proven to be very effective in dealing with a large class of high dimensional problems in computer vision (cf., e.g., [23]), natural language processing (cf., e.g., [20]), time series analysis, etc. (cf., e.g., [15, 24]). This success fuels in speculations that deep learning might hold the key to solve the curse of dimensionality problem. It should be emphasized that at the present time, there are no theoretical results that support such claims although the practical success of deep learning has been astonishing. However, this should not prevent us from trying to apply deep learning to other problems where the curse of dimensionality has been the issue.

In this paper, we explore the use of deep learning for solving general high dimensional PDEs. To this end, it is necessary to formulate the PDEs as a learning problem. Motivated by ideas in [16] where deep learning-based algorithms were developed for high dimensional stochastic control problems, we explore a connection between (nonlinear) parabolic PDEs and backward stochastic differential equations (BSDEs) (see [26, 28, 25]) since BSDEs share a lot of common features with stochastic control problems.

2 Main ideas of the algorithm

We will consider a fairly general class of nonlinear parabolic PDEs (see (30) in Subsection 4.1 below). The proposed algorithm is based on the following set of ideas:

- (i) Through the so-called nonlinear Feynman-Kac formula, we can formulate the PDEs equivalently as BSDEs.
- (ii) One can view the BSDE as a stochastic control problem with the gradient of the solution being the policy function. These stochastic control problems can then be viewed as model-based reinforcement learning problems.
- (iii) The (high dimensional) policy function can then be approximated by a deep neural network, as has been done in deep reinforcement learning.

Instead of formulating initial value problems, as is commonly done in the PDE literature, we consider the set up with terminal conditions since this facilitates making connections with BSDEs. Terminal value problems can obviously be transformed to initial value problems and vice versa.

In the remainder of this section we present a rough sketch of the derivation of the proposed algorithm, which we refer to as *deep BSDE solver*. In this derivation we restrict ourself to a specific class of nonlinear PDEs, that is, we restrict ourself to semilinear heat equations (see (PDE) below) and refer to Subsections 3.2 and 4.1 below for the general introduction of the deep BSDE solver.

2.1 An example: a semilinear heat partial differential equation (PDE)

Let $T \in (0, \infty)$, $d \in \mathbb{N}$, $\xi \in \mathbb{R}^d$, let $f: \mathbb{R} \times \mathbb{R}^d \rightarrow \mathbb{R}$ and $g: \mathbb{R}^d \rightarrow \mathbb{R}$ be continuous functions, and let $u = (u(t, x))_{t \in [0, T], x \in \mathbb{R}^d} \in C^{1,2}([0, T] \times \mathbb{R}^d, \mathbb{R})$ satisfy for all $t \in [0, T]$, $x \in \mathbb{R}^d$ that $u(T, x) = g(x)$ and

$$\frac{\partial u}{\partial t}(t, x) + \frac{1}{2}(\Delta_x u)(t, x) + f(u(t, x), (\nabla_x u)(t, x)) = 0. \quad (\text{PDE})$$

A key idea of this work is to reformulate the PDE (PDE) as an appropriate *stochastic control problem*.

2.2 Formulation of the PDE as a suitable stochastic control problem

More specifically, let $(\Omega, \mathcal{F}, \mathbb{P})$ be a probability space, let $W: [0, T] \times \Omega \rightarrow \mathbb{R}^d$ be a d -dimensional standard Brownian motion on $(\Omega, \mathcal{F}, \mathbb{P})$, let $\mathbb{F} = (\mathbb{F}_t)_{t \in [0, T]}$ be the normal filtration on $(\Omega, \mathcal{F}, \mathbb{P})$ generated by W , let \mathcal{A} be the set of all \mathbb{F} -adapted \mathbb{R}^d -valued stochastic processes with continuous sample paths, and for every $y \in \mathbb{R}$ and every $Z \in \mathcal{A}$ let $Y^{y, Z}: [0, T] \times \Omega \rightarrow \mathbb{R}$ be an \mathbb{F} -adapted stochastic process with continuous sample paths which satisfies that for all $t \in [0, T]$ it holds \mathbb{P} -a.s. that

$$Y_t^{y, Z} = y - \int_0^t f(Y_s^{y, Z}, Z_s) ds + \int_0^t \langle Z_s, dW_s \rangle_{\mathbb{R}^d}. \quad (1)$$

We now view the solution $u \in C^{1,2}([0, T] \times \mathbb{R}^d, \mathbb{R})$ of (PDE) and its spatial derivative as the solution of a stochastic control problem associated to (1). More formally, under suitable regularity hypotheses on the nonlinearity f it holds that the pair consisting of $u(0, \xi) \in \mathbb{R}$ and $((\nabla_x u)(t, \xi + W_t))_{t \in [0, T]} \in \mathcal{A}$ is the (up to indistinguishability) unique global minimum of the function

$$\mathbb{R} \times \mathcal{A} \ni (y, Z) \mapsto \mathbb{E}[|Y_T^{y, Z} - g(\xi + W_T)|^2] \in [0, \infty]. \quad (2)$$

One can also view the stochastic control problem (1)–(2) (with Z being the control) as a model-based reinforcement learning problem. In that analogy, we view Z as the policy and we approximate $Z \in \mathcal{A}$ using feedforward neural networks (see (11) and Section 4 below for further details). The process $u(t, \xi + W_t)$, $t \in [0, T]$, corresponds to the value function associated to the stochastic control problem and can be computed approximatively by employing the policy Z (see (9) below for details). The connection between the PDE (PDE) and the stochastic control problem (1)–(2) is based on the nonlinear Feynman-Kac formula which links PDEs and BSDEs (see (BSDE) and (3) below).

2.3 The nonlinear Feynman-Kac formula

Let $Y : [0, T] \times \Omega \rightarrow \mathbb{R}$ and $Z : [0, T] \times \Omega \rightarrow \mathbb{R}^d$ be \mathbb{F} -adapted stochastic processes with continuous sample paths which satisfy that for all $t \in [0, T]$ it holds \mathbb{P} -a.s. that

$$Y_t = g(\xi + W_T) + \int_t^T f(Y_s, Z_s) ds - \int_t^T \langle Z_s, dW_s \rangle_{\mathbb{R}^d}. \quad (\text{BSDE})$$

Under suitable additional regularity assumptions on the nonlinearity f we have that the nonlinear parabolic PDE (PDE) is related to the BSDE (BSDE) in the sense that for all $t \in [0, T]$ it holds \mathbb{P} -a.s. that

$$Y_t = u(t, \xi + W_t) \in \mathbb{R} \quad \text{and} \quad Z_t = (\nabla_x u)(t, \xi + W_t) \in \mathbb{R}^d \quad (3)$$

(cf., e.g., [25, Section 3] and [27]). The first identity in (3) is sometimes referred to as *nonlinear Feynman-Kac formula* in the literature.

2.4 Forward discretization of the backward stochastic differential equation (BSDE)

To derive the deep BSDE solver, we first plug the second identity in (3) into (BSDE) to obtain that for all $t \in [0, T]$ it holds \mathbb{P} -a.s. that

$$Y_t = g(\xi + W_T) + \int_t^T f(Y_s, (\nabla_x u)(s, \xi + W_s)) ds - \int_t^T \langle (\nabla_x u)(s, \xi + W_s), dW_s \rangle_{\mathbb{R}^d}. \quad (4)$$

In particular, we obtain that for all $t_1, t_2 \in [0, T]$ with $t_1 \leq t_2$ it holds \mathbb{P} -a.s. that

$$Y_{t_2} = Y_{t_1} - \int_{t_1}^{t_2} f(Y_s, (\nabla_x u)(s, \xi + W_s)) ds + \int_{t_1}^{t_2} \langle (\nabla_x u)(s, \xi + W_s), dW_s \rangle_{\mathbb{R}^d}. \quad (5)$$

Next we apply a time discretization to (5). More specifically, let $N \in \mathbb{N}$ and let $t_0, t_1, \dots, t_N \in [0, T]$ be real numbers which satisfy

$$0 = t_0 < t_1 < \dots < t_N = T \quad (6)$$

and observe that (5) suggests for $N \in \mathbb{N}$ sufficiently large that

$$\begin{aligned} Y_{t_{n+1}} & \\ \approx Y_{t_n} - f(Y_{t_n}, (\nabla_x u)(t_n, \xi + W_{t_n})) (t_{n+1} - t_n) + \langle (\nabla_x u)(t_n, \xi + W_{t_n}), W_{t_{n+1}} - W_{t_n} \rangle_{\mathbb{R}^d}. \end{aligned} \quad (7)$$

2.5 Deep learning-based approximations

In the next step we employ a deep learning approximation for

$$(\nabla_x u)(t_n, x) \in \mathbb{R}^d, \quad x \in \mathbb{R}^d, \quad n \in \{0, 1, \dots, N\}, \quad (8)$$

but not for $u(t_n, x) \in \mathbb{R}$, $x \in \mathbb{R}^d$, $n \in \{0, 1, \dots, N\}$. Approximations for $u(t_n, x) \in \mathbb{R}$, $x \in \mathbb{R}^d$, $n \in \{0, 1, \dots, N\}$, in turn, can be computed recursively by using (7) together with deep learning approximations for (8). More specifically, let $\rho \in \mathbb{N}$, let $\mathcal{U}^\theta \in \mathbb{R}$, $\theta \in \mathbb{R}^\rho$, be real numbers, let $\mathcal{V}_n^\theta: \mathbb{R}^d \rightarrow \mathbb{R}^d$, $n \in \{0, 1, \dots, N-1\}$, $\theta \in \mathbb{R}^\rho$, be continuous functions, and let $\mathcal{Y}^\theta: \{0, 1, \dots, N\} \times \Omega \rightarrow \mathbb{R}$, $\theta \in \mathbb{R}^\rho$, be stochastic processes which satisfy for all $\theta \in \mathbb{R}^\rho$, $n \in \{0, 1, \dots, N-1\}$ that $\mathcal{Y}_0^\theta = \mathcal{U}^\theta$ and

$$\mathcal{Y}_{n+1}^\theta = \mathcal{Y}_n^\theta - f(\mathcal{Y}_n^\theta, \mathcal{V}_n^\theta(\xi + W_{t_n})) (t_{n+1} - t_n) + \langle \mathcal{V}_n^\theta(\xi + W_{t_n}), W_{t_{n+1}} - W_{t_n} \rangle_{\mathbb{R}^d}. \quad (9)$$

We think of $\rho \in \mathbb{N}$ as the number of parameters in the neural network, for all appropriate $\theta \in \mathbb{R}^\rho$ we think of $\mathcal{U}^\theta \in \mathbb{R}$ as suitable approximations

$$\mathcal{U}^\theta \approx u(0, \xi) \quad (10)$$

of $u(0, \xi)$, and for all appropriate $\theta \in \mathbb{R}^\rho$, $x \in \mathbb{R}^d$, $n \in \{0, 1, \dots, N-1\}$ we think of $\mathcal{V}_n^\theta(x) \in \mathbb{R}^{1 \times d}$ as suitable approximations

$$\mathcal{V}_n^\theta(x) \approx (\nabla_x u)(t_n, x) \quad (11)$$

of $(\nabla_x u)(t_n, x)$.

2.6 Stochastic optimization algorithms

The ‘‘appropriate’’ $\theta \in \mathbb{R}^\rho$ can be obtained by minimizing the expected loss function through stochastic gradient descent-type algorithms. For the loss function we pick the squared approximation error associated to the terminal condition of the BSDE (BSDE). More precisely, assume that the function $\mathbb{R}^\rho \ni \theta \mapsto \mathbb{E}[|\mathcal{Y}_N^\theta - g(\mathcal{X}_N)|^2] \in [0, \infty]$ has a unique global minimum and let $\Lambda \in \mathbb{R}^\rho$ be the real vector for which the function

$$\mathbb{R}^\rho \ni \theta \mapsto \mathbb{E}[|\mathcal{Y}_N^\theta - g(\mathcal{X}_N)|^2] \in [0, \infty] \quad (12)$$

is minimal. Minimizing the function (12) is inspired by the fact that

$$\mathbb{E}[|Y_T - g(X_T)|^2] = 0 \quad (13)$$

according to (BSDE) above (cf. (2) above). Under suitable regularity assumptions, we approximate the vector $\Lambda \in \mathbb{R}^\rho$ through stochastic gradient descent-type approximation methods and thereby we obtain random approximations $\Theta_0, \Theta_1, \Theta_2, \dots : \Omega \rightarrow \mathbb{R}^\rho$ of $\Lambda \in \mathbb{R}^\rho$. For sufficiently large $N, \rho, m \in \mathbb{N}$ we then employ the random variable $\mathcal{U}^{\Theta_m} : \Omega \rightarrow \mathbb{R}$ as a suitable implementable approximation

$$\mathcal{U}^{\Theta_m} \approx u(0, \xi) \quad (14)$$

of $u(0, \xi)$ (cf. (10) above) and for sufficiently large $N, \rho, m \in \mathbb{N}$ and all $x \in \mathbb{R}^d$, $n \in \{0, 1, \dots, N-1\}$ we use the random variable $\mathcal{V}_n^{\Theta_m}(x) : \Omega \rightarrow \mathbb{R}^{1 \times d}$ as a suitable implementable approximation

$$\mathcal{V}_n^{\Theta_m}(x) \approx (\nabla_x u)(t_n, x) \quad (15)$$

of $(\nabla_x u)(t_n, x)$ (cf. (11) above). In the next section the proposed approximation method is described in more detail.

To simplify the presentation we have restricted us in (PDE), (1), (2), (BSDE) above and Subsection 3.1 below to semilinear heat equations. We refer to Subsection 3.2 and Section 4 below for the general description of the deep BSDE solver.

3 Details of the algorithm

3.1 Formulation of the proposed algorithm in the case of semilinear heat equations

In this subsection we describe the algorithm proposed in this article in the specific situation where (PDE) is the PDE under consideration, where *batch normalization* (see Ioffe & Szegedy [21]) is not employed, and where the plain-vanilla stochastic gradient descent approximation method with a constant learning rate $\gamma \in (0, \infty)$ and without mini-batches is the employed stochastic algorithm. The general framework, which includes the setting in this subsection as a special case, can be found in Subsection 3.2 below.

Framework 3.1 (Specific case). *Let $T, \gamma \in (0, \infty)$, $d, \rho, N \in \mathbb{N}$, $\xi \in \mathbb{R}^d$, let $f : \mathbb{R} \times \mathbb{R}^d \rightarrow \mathbb{R}$ and $g : \mathbb{R}^d \rightarrow \mathbb{R}$ be functions, let $(\Omega, \mathcal{F}, \mathbb{P})$ be a probability space, let $W^m : [0, T] \times \Omega \rightarrow \mathbb{R}^d$, $m \in \mathbb{N}_0$, be independent d -dimensional standard Brownian motions on $(\Omega, \mathcal{F}, \mathbb{P})$, let $t_0, t_1, \dots, t_N \in [0, T]$ be real numbers with*

$$0 = t_0 < t_1 < \dots < t_N = T, \quad (16)$$

for every $\theta \in \mathbb{R}^\rho$ let $\mathcal{U}^\theta \in \mathbb{R}$, for every $\theta \in \mathbb{R}^\rho$, $n \in \{0, 1, \dots, N-1\}$ let $\mathcal{V}_n^\theta : \mathbb{R}^d \rightarrow \mathbb{R}^d$ be a function, for every $m \in \mathbb{N}_0$, $\theta \in \mathbb{R}^\rho$ let $\mathcal{Y}^{\theta, m} : \{0, 1, \dots, N\} \times \Omega \rightarrow \mathbb{R}^k$ be the stochastic process which satisfies for all $n \in \{0, 1, \dots, N-1\}$ that $\mathcal{Y}_0^{\theta, m} = \mathcal{U}^\theta$ and

$$\mathcal{Y}_{n+1}^{\theta, m} = \mathcal{Y}_n^{\theta, m} - f(\mathcal{Y}_n^{\theta, m}, \mathcal{V}_n^\theta(\xi + W_{t_n}^m))(t_{n+1} - t_n) + \langle \mathcal{V}_n^\theta(\xi + W_{t_n}^m), W_{t_{n+1}}^m - W_{t_n}^m \rangle_{\mathbb{R}^d}, \quad (17)$$

for every $m \in \mathbb{N}_0$ let $\phi^m: \mathbb{R}^\rho \times \Omega \rightarrow \mathbb{R}$ be the function which satisfies for all $\theta \in \mathbb{R}^\rho$, $\omega \in \Omega$ that

$$\phi^m(\theta, \omega) = |\mathcal{Y}_N^{\theta, m}(\omega) - g(\xi + W_T^m(\omega))|^2, \quad (18)$$

for every $m \in \mathbb{N}_0$ let $\Phi^m: \mathbb{R}^\rho \times \Omega \rightarrow \mathbb{R}^\rho$ be a function which satisfies for all $\omega \in \Omega$, $\theta \in \{v \in \mathbb{R}^\rho: (\mathbb{R}^\rho \ni w \mapsto \phi_s^m(w, \omega) \in \mathbb{R} \text{ is differentiable at } v \in \mathbb{R}^\rho)\}$ that

$$\Phi^m(\theta, \omega) = (\nabla_\theta \phi^m)(\theta, \omega), \quad (19)$$

and let $\Theta: \mathbb{N}_0 \times \Omega \rightarrow \mathbb{R}^\rho$ be a stochastic process which satisfy for all $m \in \mathbb{N}$ that

$$\Theta_m = \Theta_{m-1} - \gamma \cdot \Phi^m(\Theta_{m-1}). \quad (20)$$

Under suitable further hypotheses (cf. Sections 4 and 5 below), we think in the case of sufficiently large $\rho, N, m \in \mathbb{N}$ and sufficiently small $\gamma \in (0, \infty)$ of $\mathcal{U}^{\Theta_m} \in \mathbb{R}$ as an appropriate approximation

$$u(0, \xi) \approx \mathcal{U}^{\Theta_m} \quad (21)$$

of the solution $u(t, x) \in \mathbb{R}$, $(t, x) \in [0, T] \times \mathbb{R}^d$, of the PDE

$$\frac{\partial u}{\partial t}(t, x) + \frac{1}{2}(\Delta_x u)(t, x) + f(u(t, x), (\nabla_x u)(t, x)) = 0 \quad (22)$$

for $(t, x) \in [0, T] \times \mathbb{R}^d$.

3.2 Formulation of the proposed algorithm in the general case

Framework 3.2 (General case). Let $T \in (0, \infty)$, $d, k, \rho, \varrho, N, \varsigma \in \mathbb{N}$, $\xi \in \mathbb{R}^d$, let $f: [0, T] \times \mathbb{R}^d \times \mathbb{R}^k \times \mathbb{R}^{k \times d} \rightarrow \mathbb{R}$, $g: \mathbb{R}^d \rightarrow \mathbb{R}^k$, and $\Upsilon: [0, T]^2 \times \mathbb{R}^d \times \mathbb{R}^d \rightarrow \mathbb{R}^d$ be functions, let $(\Omega, \mathcal{F}, \mathbb{P})$ be a probability space, let $W^{m, j}: [0, T] \times \Omega \rightarrow \mathbb{R}^d$, $m, j \in \mathbb{N}_0$, be independent d -dimensional standard Brownian motions on $(\Omega, \mathcal{F}, \mathbb{P})$, let $t_0, t_1, \dots, t_N \in [0, T]$ be real numbers with

$$0 = t_0 < t_1 < \dots < t_N = T, \quad (23)$$

for every $\theta \in \mathbb{R}^\rho$ let $\mathcal{U}^\theta \in \mathbb{R}^k$, for every $\theta \in \mathbb{R}^\rho$, $\mathbf{s} \in \mathbb{R}^\varsigma$, $n \in \{0, 1, \dots, N-1\}$, $j \in \mathbb{N}_0$ let $\mathcal{V}_{n, j}^{\theta, \mathbf{s}}: (\mathbb{R}^d)^{\mathbb{N}} \rightarrow \mathbb{R}^{k \times d}$ be a function, for every $m, j \in \mathbb{N}_0$ let $\mathcal{X}^{m, j}: \{0, 1, \dots, N\} \times \Omega \rightarrow \mathbb{R}^d$ and $\mathcal{Y}^{\theta, \mathbf{s}, m, j}: \{0, 1, \dots, N\} \times \Omega \rightarrow \mathbb{R}^k$, $\theta \in \mathbb{R}^\rho$, $\mathbf{s} \in \mathbb{R}^\varsigma$, be stochastic processes which satisfy for all $\theta \in \mathbb{R}^\rho$, $\mathbf{s} \in \mathbb{R}^\varsigma$, $n \in \{0, 1, \dots, N-1\}$ that

$$\mathcal{X}_0^{m, j} = \xi, \quad \mathcal{Y}_0^{\theta, \mathbf{s}, m, j} = \mathcal{U}^\theta, \quad \mathcal{X}_{n+1}^{m, j} = \Upsilon(t_n, t_{n+1}, \mathcal{X}_n^{m, j}, W_{t_{n+1}}^{m, j} - W_{t_n}^{m, j}), \quad (24)$$

$$\begin{aligned} \mathcal{Y}_{n+1}^{\theta, \mathbf{s}, m, j} &= \mathcal{Y}_n^{\theta, \mathbf{s}, m, j} - f(t_n, \mathcal{X}_n^{m, j}, \mathcal{Y}_n^{\theta, \mathbf{s}, m, j}, \mathcal{V}_{n, j}^{\theta, \mathbf{s}}(\{\mathcal{X}_n^{m, i}\}_{i \in \mathbb{N}})) (t_{n+1} - t_n) \\ &\quad + \mathcal{V}_{n, j}^{\theta, \mathbf{s}}(\{\mathcal{X}_n^{m, i}\}_{i \in \mathbb{N}}) (W_{t_{n+1}}^{m, j} - W_{t_n}^{m, j}), \end{aligned} \quad (25)$$

for every $m, j \in \mathbb{N}_0$, $\mathbf{s} \in \mathbb{R}^\zeta$ let $\phi_{\mathbf{s}}^{m,j}: \mathbb{R}^\rho \times \Omega \rightarrow \mathbb{R}$ be the function which satisfies for all $\theta \in \mathbb{R}^\rho$, $\omega \in \Omega$ that

$$\phi_{\mathbf{s}}^{m,j}(\theta, \omega) = \|\mathcal{Y}_N^{\theta, \mathbf{s}, m, j}(\omega) - g(\mathcal{X}_N^{m,j}(\omega))\|_{\mathbb{R}^k}^2, \quad (26)$$

for every $m, j \in \mathbb{N}_0$, $\mathbf{s} \in \mathbb{R}^\zeta$ let $\Phi_{\mathbf{s}}^{m,j}: \mathbb{R}^\rho \times \Omega \rightarrow \mathbb{R}^\rho$ be a function which satisfies for all $\omega \in \Omega$, $\theta \in \{v \in \mathbb{R}^\rho: (\mathbb{R}^\rho \ni w \mapsto \phi_{\mathbf{s}}^{m,j}(w, \omega) \in \mathbb{R} \text{ is differentiable at } v \in \mathbb{R}^\rho)\}$ that

$$\Phi_{\mathbf{s}}^{m,j}(\theta, \omega) = (\nabla_{\theta} \phi_{\mathbf{s}}^{m,j})(\theta, \omega), \quad (27)$$

let $\mathcal{S}: \mathbb{R}^\zeta \times \mathbb{R}^\rho \times (\mathbb{R}^d)^{\{0,1,\dots,N-1\} \times \mathbb{N}} \rightarrow \mathbb{R}^\zeta$ be a function, for every $m \in \mathbb{N}$ let $\psi_m: \mathbb{R}^\rho \rightarrow \mathbb{R}^\rho$ and $\Psi_m: \mathbb{R}^\rho \times (\mathbb{R}^\rho)^{\mathbb{N}} \rightarrow \mathbb{R}^\rho$ be functions, and let $\mathbb{S}: \mathbb{N}_0 \times \Omega \rightarrow \mathbb{R}^\zeta$, $\Xi: \mathbb{N}_0 \times \Omega \rightarrow \mathbb{R}^\rho$, and $\Theta: \mathbb{N}_0 \times \Omega \rightarrow \mathbb{R}^\rho$ be stochastic processes which satisfy for all $m \in \mathbb{N}$ that

$$\mathbb{S}_m = \mathcal{S}(\mathbb{S}_{m-1}, \Theta_{m-1}, \{\mathcal{X}_n^{m-1,i}\}_{(n,i) \in \{0,1,\dots,N-1\} \times \mathbb{N}}), \quad (28)$$

$$\Xi_m = \Psi_m(\Xi_{m-1}, \{\Phi_{\mathbb{S}_m}^{m-1,j}(\Theta_{m-1})\}_{j \in \mathbb{N}}), \quad \text{and} \quad \Theta_m = \Theta_{m-1} - \psi_m(\Xi_m). \quad (29)$$

3.3 Comments on the proposed algorithm

The dynamics in (24) associated to the stochastic processes $(\mathcal{X}_n^{m,j})_{n \in \{0,1,\dots,N\}}$ for $m, j \in \mathbb{N}_0$ allows us to incorporate different algorithms for the discretization of the considered forward stochastic differential equation (SDE) into the deep BSDE solver in Subsection 3.2. The dynamics in (29) associated to the stochastic processes Ξ_m , $m \in \mathbb{N}_0$, and Θ_m , $m \in \mathbb{N}_0$, allows us to incorporate different stochastic approximation algorithms such as

- stochastic gradient descent with or without mini-batches (see Subsection 5.1 below) as well as
- adaptive moment estimation (Adam) with mini-batches (see Kingma & Jimmy [22] and Subsection 5.2 below) into the deep BSDE solver in Subsection 3.2.

The dynamics in (28) associated to the stochastic process \mathbb{S}_m , $m \in \mathbb{N}_0$, allows us to incorporate the standardization procedure in *batch normalization* (see Ioffe & Szegedy [21] and also Section 4 below) into the deep BSDE solver in Subsection 3.2. In that case we think of \mathbb{S}_m , $m \in \mathbb{N}_0$, as approximatively calculated means and standard deviations.

4 Examples for nonlinear partial differential equations (PDEs) and nonlinear backward stochastic differential equations (BSDEs)

In this section we illustrate the algorithm proposed in Subsection 3.2 using several concrete example PDEs. In the examples below we will employ the general approximation

method in Subsection 3.2 in conjunction with the Adam optimizer (cf. Example 5.2 below and Kingma & Ba [22]) with mini-batches with 64 samples in each iteration step (see Subsection 4.1 for a detailed description).

In our implementation we employ $N - 1$ fully-connected feedforward neural networks to represent $\mathcal{V}_{n,j}^\theta$ for $n \in \{1, 2, \dots, N - 1\}$, $j \in \{1, 2, \dots, 64\}$, $\theta \in \mathbb{R}^\rho$ (cf. also Figure 1 below for a rough sketch of the architecture of the deep BSDE solver). Each of the neural networks consists of 4 layers (1 input layer [d -dimensional], 2 hidden layers [both $d + 10$ -dimensional], and 1 output layer [d -dimensional]). The number of hidden units in each hidden layer is equal to $d + 10$. We also adopt batch normalization (BN) (see Ioffe & Szegedy [21]) right after each matrix multiplication and before activation. We employ the rectifier function $\mathbb{R} \ni x \mapsto \max\{0, x\} \in [0, \infty)$ as our activation function for the hidden variables. All the weights in the network are initialized using a normal or a uniform distribution without any pre-training. Each of the numerical experiments presented below is performed in PYTHON using TENSORFLOW on a MACBOOK PRO with a 2.90 Gigahertz (GHz) INTEL CORE i5 micro processor and 16 gigabytes (GB) of 1867 Megahertz (MHz) double data rate type three synchronous dynamic random-access memory (DDR3-SDRAM). We also refer to the PYTHON code 1 in Subsection 6.1 below for an implementation of the deep BSDE solver in the case of the 100-dimensional Allen-Cahn PDE (35).

4.1 Setting

Assume the setting in Subsection 3.2, assume for all $\theta = (\theta_1, \dots, \theta_\rho) \in \mathbb{R}^\rho$ that $k = 1$, $\rho = d + 1 + (N - 1)(2d(d + 10) + (d + 10)^2 + 4(d + 10) + 2d)$, $\varrho = 2\rho$, $\mathcal{U}^\theta = \theta_1$, $\Xi_0 = 0$, let $\mu: [0, T] \times \mathbb{R}^d \rightarrow \mathbb{R}^d$ and $\sigma: [0, T] \times \mathbb{R}^d \rightarrow \mathbb{R}^{d \times d}$ be functions, let $u: [0, T] \times \mathbb{R}^d \rightarrow \mathbb{R}$ be a continuous and at most polynomially growing function which satisfies for all $(t, x) \in [0, T] \times \mathbb{R}^d$ that $u|_{[0, T] \times \mathbb{R}^d} \in C^{1,2}([0, T] \times \mathbb{R}^d, \mathbb{R})$, $u(T, x) = g(x)$, and

$$\begin{aligned} \frac{\partial u}{\partial t}(t, x) + \frac{1}{2} \text{Trace}(\sigma(t, x) [\sigma(t, x)]^* (\text{Hess}_x u)(t, x)) + \langle \mu(t, x), (\nabla_x u)(t, x) \rangle \\ + f(t, x, u(t, x), [(\nabla_x u)(t, x)]^* \sigma(t, x)) = 0, \end{aligned} \quad (30)$$

let $\varepsilon = 10^{-8}$, $\mathbb{X} = \frac{9}{10}$, $\mathbb{Y} = \frac{999}{1000}$, $J = 64$, $(\gamma_m)_{m \in \mathbb{N}} \subseteq (0, \infty)$, let $\text{Pow}_r: \mathbb{R}^\rho \rightarrow \mathbb{R}^\rho$, $r \in (0, \infty)$, be the functions which satisfy for all $r \in (0, \infty)$, $x = (x_1, \dots, x_\rho) \in \mathbb{R}^\rho$ that

$$\text{Pow}_r(x) = (|x_1|^r, \dots, |x_\rho|^r), \quad (31)$$

and assume for all $m \in \mathbb{N}$, $x, y \in \mathbb{R}^\rho$, $(\varphi_j)_{j \in \mathbb{N}} \in (\mathbb{R}^\rho)^\mathbb{N}$ that

$$\Psi_m(x, y, (\varphi_j)_{j \in \mathbb{N}}) = (\mathbb{X}x + (1 - \mathbb{X})\left(\frac{1}{J} \sum_{j=1}^J \varphi_j\right), \mathbb{Y}y + (1 - \mathbb{Y})\text{Pow}_2\left(\frac{1}{J} \sum_{j=1}^J \varphi_j\right)) \quad (32)$$

and

$$\psi_m(x, y) = \left[\varepsilon + \text{Pow}_{1/2} \left(\frac{y}{(1 - \mathbb{Y}^m)} \right) \right]^{-1} \frac{\gamma_m x}{(1 - \mathbb{X}^m)}. \quad (33)$$

(cf. Example 5.2 below and Kingma & Ba [22]).

Remark 4.1. *In this remark we illustrate the specific choice of the dimension $\rho \in \mathbb{N}$ of $\theta = (\theta_1, \dots, \theta_\rho) \in \mathbb{R}^\rho$ in the framework in Subsection 4.1 above.*

- (i) *The first component of $\theta = (\theta_1, \dots, \theta_\rho) \in \mathbb{R}^\rho$ is employed for approximating the real number $u(0, \xi) \in \mathbb{R}$.*
- (ii) *The next d -components of $\theta = (\theta_1, \dots, \theta_\rho) \in \mathbb{R}^\rho$ are employed for approximating the components of the $(1 \times d)$ -matrix $(\frac{\partial}{\partial x}u)(0, \xi) \sigma(0, \xi) \in \mathbb{R}^{1 \times d}$.*
- (iii) *In each of the employed $N - 1$ neural networks we use $d(d + 10)$ components of $\theta = (\theta_1, \dots, \theta_\rho) \in \mathbb{R}^\rho$ to describe the linear transformation from the d -dimensional first layer (input layer) to the $(d + 10)$ -dimensional second layer (first hidden layer) (to uniquely describe a real $(d + 10) \times d$ -matrix).*
- (iv) *In each of the employed $N - 1$ neural networks we use $(d + 10)^2$ components of $\theta = (\theta_1, \dots, \theta_\rho) \in \mathbb{R}^\rho$ to uniquely describe the linear transformation from the $(d + 10)$ -dimensional second layer (first hidden layer) to the $(d + 10)$ -dimensional third layer (second hidden layer) (to uniquely describe a real $(d + 10) \times (d + 10)$ -matrix).*
- (v) *In each of the employed $N - 1$ neural networks we use $d(d + 10)$ components of $\theta = (\theta_1, \dots, \theta_\rho) \in \mathbb{R}^\rho$ to describe the linear transformation from the $(d + 10)$ -dimensional third layer (second hidden layer) to the d -dimensional fourth layer (output layer) (to uniquely describe a real $d \times (d + 10)$ -matrix).*
- (vi) *After each of the linear transformations in items (iii)–(v) above we employ a componentwise affine linear transformation (multiplication with a diagonal matrix and addition of a vector) within the batch normalization procedure, i.e., in each of the employed $N - 1$ neural networks, we use $2(d + 10)$ components of $\theta = (\theta_1, \dots, \theta_\rho) \in \mathbb{R}^\rho$ for the componentwise affine linear transformation between the first linear transformation (see item (iii)) and the first application of the activation function, we use $2(d + 10)$ components of $\theta = (\theta_1, \dots, \theta_\rho) \in \mathbb{R}^\rho$ for the componentwise affine linear transformation between the second linear transformation (see item (iv)) and the second application of the activation function, and we use $2d$ components of $\theta = (\theta_1, \dots, \theta_\rho) \in \mathbb{R}^\rho$ for the componentwise affine linear transformation after the third linear transformation (see item (v)).*

Summing (i)–(vi) results in

$$\begin{aligned}
\rho &= \underbrace{1 + d}_{\text{items (i)–(ii)}} + \underbrace{(N - 1) (d(d + 10) + (d + 10)^2 + d(d + 10))}_{\text{items (iii)–(v)}} \\
&\quad + \underbrace{(N - 1) (2(d + 10) + 2(d + 10) + 2d)}_{\text{item (vi)}} \tag{34} \\
&= d + 1 + (N - 1) (2d(d + 10) + (d + 10)^2 + 4(d + 10) + 2d) .
\end{aligned}$$

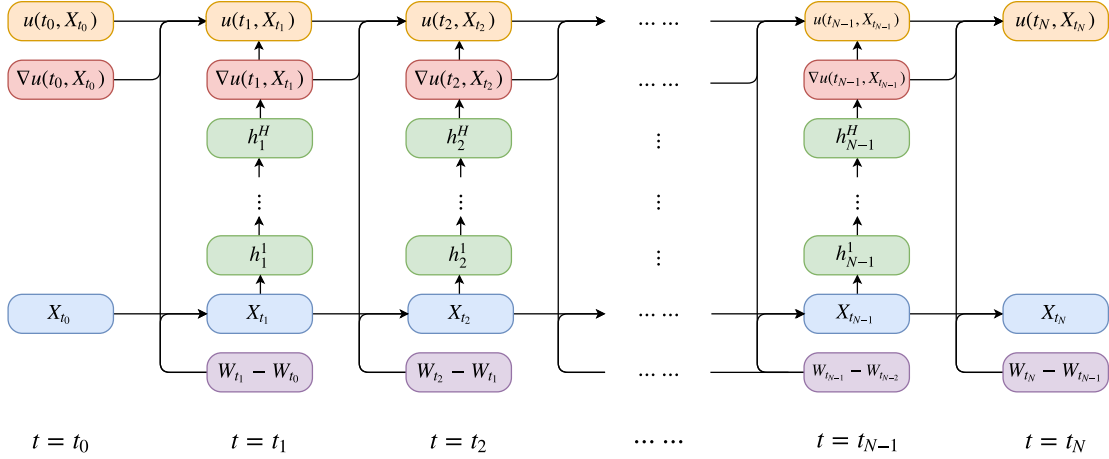


Figure 1: Rough sketch of the architecture of the deep BSDE solver.

4.2 Allen-Cahn equation

In this section we test the deep BSDE solver in the case of an 100-dimensional Allen-Cahn PDE with a cubic nonlinearity (see (35) below).

More specifically, assume the setting in the Subsection 4.1 and assume for all $s, t \in [0, T]$, $x, w \in \mathbb{R}^d$, $y \in \mathbb{R}$, $z \in \mathbb{R}^{1 \times d}$, $m \in \mathbb{N}$ that $\gamma_m = 5 \cdot 10^{-4}$, $d = 100$, $T = \frac{3}{10}$, $N = 20$, $\mu(t, x) = 0$, $\sigma(t, x)w = \sqrt{2}w$, $\xi = (0, 0, \dots, 0) \in \mathbb{R}^d$, $\Upsilon(s, t, x, w) = x + \sqrt{2}w$, $f(t, x, y, z) = y - y^3$, and $g(x) = [2 + \frac{2}{5} \|x\|_{\mathbb{R}^d}^2]^{-1}$. Note that the solution u of the PDE (30) then satisfies for all $t \in [0, T)$, $x \in \mathbb{R}^d$ that $u(T, x) = g(x)$ and

$$\frac{\partial u}{\partial t}(t, x) + u(t, x) - [u(t, x)]^3 + (\Delta_x u)(t, x) = 0. \quad (35)$$

In Table 1 we approximatively calculate the mean of \mathcal{U}^{Θ_m} , the standard deviation of \mathcal{U}^{Θ_m} , the relative L^1 -approximation error associated to \mathcal{U}^{Θ_m} , the standard deviation of the relative L^1 -approximation error associated to \mathcal{U}^{Θ_m} , and the runtime in seconds needed to calculate one realization of \mathcal{U}^{Θ_m} against $m \in \{0, 1000, 2000, 3000, 4000\}$ based on 5 independent realizations (5 independent runs) (see also the PYTHON code 1 below). Table 1 also depicts the mean of the loss function associated to Θ_m and the standard deviation of the loss function associated to Θ_m against $m \in \{0, 1000, 2000, 3000, 4000\}$ based on 256 Monte Carlo samples and 5 independent realizations (5 independent runs). In addition, the relative L^1 -approximation error associated to \mathcal{U}^{Θ_m} against $m \in \{1, 2, 3, \dots, 4000\}$ is pictured on the left hand side of Figure 2 based on 5 independent realizations (5 independent runs) and the mean of the loss function associated to Θ_m against $m \in \{1, 2, 3, \dots, 4000\}$ is pictured on the right hand side of Figure 2 based on 256 Monte Carlo samples and 5 independent realizations (5 independent runs). In the approximative computations of the relative L^1 -

approximation errors in Table 1 and Figure 2 the value $u(0, \xi) = u(0, 0, \dots, 0)$ of the exact solution u of the PDE (35) is replaced by the value 0.052802 which, in turn, is calculated by means of the Branching diffusion method (see the MATLAB code 2 below and see, e.g., [17, 19, 18] for analytical and numerical results for the Branching diffusion method in the literature).

Number of iteration steps m	Mean of \mathcal{U}^{Θ_m}	Standard deviation of \mathcal{U}^{Θ_m}	Relative L^1 -appr. error	Standard deviation of the relative L^1 -appr. error	Mean of the loss function	Standard deviation of the loss function	Runtime in sec. for one realization of \mathcal{U}^{Θ_m}
0	0.4740	0.0514	7.9775	0.9734	0.11630	0.02953	
1000	0.1446	0.0340	1.7384	0.6436	0.00550	0.00344	201
2000	0.0598	0.0058	0.1318	0.1103	0.00029	0.00006	348
3000	0.0530	0.0002	0.0050	0.0041	0.00023	0.00001	500
4000	0.0528	0.0002	0.0030	0.0022	0.00020	0.00001	647

Table 1: Numerical simulations for the deep BSDE solver in Subsection 3.2 in the case of the PDE (35).

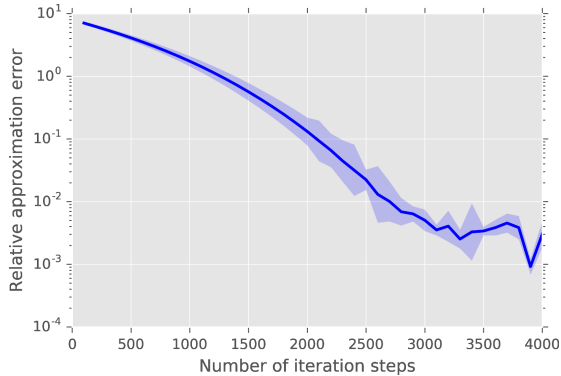
4.3 A Hamilton-Jacobi-Bellman (HJB) equation

In this subsection we apply the deep BSDE solver in Subsection 3.2 to a Hamilton-Jacobi-Bellman (HJB) equation which admits an explicit solution that can be obtained through the Cole-Hopf transformation (cf., e.g., Chassagneux & Richou [7, Section 4.2] and Debnath [10, Section 8.4]).

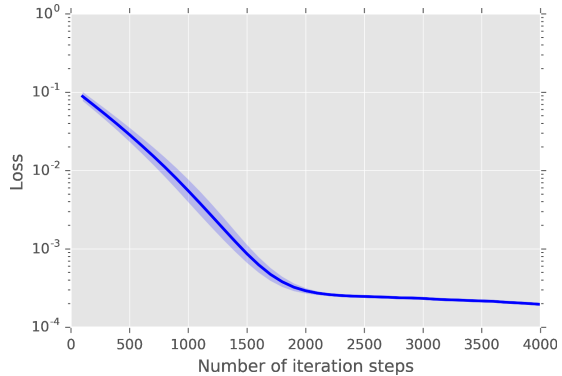
Assume the setting in the Subsection 4.1 and assume for all $s, t \in [0, T]$, $x, w \in \mathbb{R}^d$, $y \in \mathbb{R}$, $z \in \mathbb{R}^{1 \times d}$, $m \in \mathbb{N}$ that $d = 100$, $T = 1$, $N = 20$, $\gamma_m = \frac{1}{100}$, $\mu(t, x) = 0$, $\sigma(t, x)w = \sqrt{2}w$, $\xi = (0, 0, \dots, 0) \in \mathbb{R}^d$, $\Upsilon(s, t, x, w) = x + \sqrt{2}w$, $f(t, x, y, z) = -\|z\|_{\mathbb{R}^{1 \times d}}^2$, and $g(x) = \ln(\frac{1}{2} [1 + \|x\|_{\mathbb{R}^d}^2])$. Note that the solution u of the PDE (30) then satisfies for all $t \in [0, T]$, $x \in \mathbb{R}^d$ that $u(T, x) = g(x)$ and

$$\frac{\partial u}{\partial t}(t, x) + (\Delta_x u)(t, x) = \|(\nabla_x u)(t, x)\|_{\mathbb{R}^d}^2. \quad (36)$$

In Table 2 we approximatively calculate the mean of \mathcal{U}^{Θ_m} , the standard deviation of \mathcal{U}^{Θ_m} , the relative L^1 -approximatin error associated to \mathcal{U}^{Θ_m} , the standard deviation of the relative L^1 -approximatin error associated to \mathcal{U}^{Θ_m} , and the runtime in seconds needed to



(a) Relative L^1 -approximation error



(b) Mean of the loss function

Figure 2: Relative L^1 -approximation error of \mathcal{U}^{Θ_m} and mean of the loss function against $m \in \{1, 2, 3, \dots, 4000\}$ in the case of the PDE (35). The deep BSDE approximation $\mathcal{U}^{\Theta_{4000}} \approx u(0, \xi)$ achieves a relative L^1 -approximation error of size 0.0030 in a runtime of 595 seconds.

calculate one realization of \mathcal{U}^{Θ_m} against $m \in \{0, 500, 1000, 1500, 2000\}$ based on 5 independent realizations (5 independent runs). Table 2 also depicts the mean of the loss function associated to Θ_m and the standard deviation of the loss function associated to Θ_m against $m \in \{0, 500, 1000, 1500, 2000\}$ based on 256 Monte Carlo samples and 5 independent realizations (5 independent runs). In addition, the relative L^1 -approximation error associated to \mathcal{U}^{Θ_m} against $m \in \{1, 2, 3, \dots, 2000\}$ is pictured on the left hand side of Figure 3 based on 5 independent realizations (5 independent runs) and the mean of the loss function associated to Θ_m against $m \in \{1, 2, 3, \dots, 2000\}$ is pictured on the right hand side of Figure 3 based on 256 Monte Carlo samples and 5 independent realizations (5 independent runs). In the approximative computations of the relative L^1 -approximation errors in Table 2 and Figure 3 the value $u(0, \xi) = u(0, 0, \dots, 0)$ of the exact solution u of the PDE (35) is replaced by the value 4.5901 which, in turn, is calculated by means of Lemma 4.2 below (with $d = 100$, $T = 1$, $\alpha = 1$, $\beta = -1$, $g = \mathbb{R}^d \ni x \mapsto \ln(\frac{1}{2}[1 + \|x\|_{\mathbb{R}^d}^2]) \in \mathbb{R}$ in the notation of Lemma 4.2) and a classical Monte Carlo method (see the MATLAB code 3 below).

Lemma 4.2 (Cf., e.g., Section 4.2 in [7] and Section 8.4 in [10]). *Let $d \in \mathbb{N}$, $T, \alpha \in (0, \infty)$, $\beta \in \mathbb{R} \setminus \{0\}$, let $(\Omega, \mathcal{F}, \mathbb{P})$ be a probability space, let $W: [0, T] \times \Omega \rightarrow \mathbb{R}^d$ be a d -dimensional standard Brownian motion, let $g \in C^2(\mathbb{R}^d, \mathbb{R})$ be a function which satisfies $\sup_{x \in \mathbb{R}^d} [\beta g(x)] < \infty$, let $f: [0, T] \times \mathbb{R}^d \times \mathbb{R} \times \mathbb{R}^d \rightarrow \mathbb{R}$ be the function which satisfies for all $t \in [0, T]$, $x = (x_1, \dots, x_d), z = (z_1, \dots, z_d) \in \mathbb{R}^d$, $y \in \mathbb{R}$ that*

$$f(t, x, y, z) = \beta \|z\|_{\mathbb{R}^d}^2 = \beta \sum_{i=1}^d |z_i|^2, \quad (37)$$

Number of iteration steps m	Mean of \mathcal{U}^{Θ_m}	Standard deviation of \mathcal{U}^{Θ_m}	Relative L^1 -appr. error	Standard deviation of the relative L^1 -appr. error	Mean of the loss function	Standard deviation of the loss function	Runtime in sec. for one realization of \mathcal{U}^{Θ_m}
0	0.3167	0.3059	0.9310	0.0666	18.4052	2.5090	
500	2.2785	0.3521	0.5036	0.0767	2.1789	0.3848	116
1000	3.9229	0.3183	0.1454	0.0693	0.5226	0.2859	182
1500	4.5921	0.0063	0.0013	0.006	0.0239	0.0024	248
2000	4.5977	0.0019	0.0017	0.0004	0.0231	0.0026	330

Table 2: Numerical simulations for the deep BSDE solver in Subsection 3.2 in the case of the PDE (36).

and let $u: [0, T] \times \mathbb{R}^d \rightarrow \mathbb{R}$ be the function which satisfies for all $(t, x) \in [0, T] \times \mathbb{R}^d$ that

$$u(t, x) = \frac{\alpha}{\beta} \ln \left(\mathbb{E} \left[\exp \left(\frac{\beta g(x + W_{T-t} \sqrt{2\alpha})}{\alpha} \right) \right] \right). \quad (38)$$

Then

- (i) it holds that $u: [0, T] \times \mathbb{R}^d \rightarrow \mathbb{R}$ is a continuous function,
- (ii) it holds that $u|_{[0, T] \times \mathbb{R}^d} \in C^{1,2}([0, T] \times \mathbb{R}^d, \mathbb{R})$, and
- (iii) it holds for all $(t, x) \in [0, T] \times \mathbb{R}^d$ that $u(T, x) = g(x)$ and

$$\begin{aligned} & \frac{\partial u}{\partial t}(t, x) + \alpha(\Delta_x u)(t, x) + f(t, x, u(t, x), (\nabla_x u)(t, x)) \\ &= \frac{\partial u}{\partial t}(t, x) + \alpha(\Delta_x u)(t, x) + \beta \|(\nabla_x u)(t, x)\|_{\mathbb{R}^d}^2 \\ &= \frac{\partial u}{\partial t}(t, x) + \alpha(\Delta_x u)(t, x) + \beta \sum_{j=1}^d \left| \frac{\partial u}{\partial x_j}(t, x) \right|^2 = 0. \end{aligned} \quad (39)$$

Proof of Lemma 4.2. Throughout this proof let $c = \frac{\alpha}{\beta} \in \mathbb{R} \setminus \{0\}$ and let $\mathcal{V}: \mathbb{R}^d \rightarrow (0, \infty)$ and $v: [0, T] \times \mathbb{R}^d \rightarrow (0, \infty)$ be the functions which satisfy for all $t \in [0, T]$, $x \in \mathbb{R}^d$ that

$$\mathcal{V}(x) = \exp\left(\frac{g(x)}{c}\right) = \exp\left(\frac{\beta g(x)}{\alpha}\right) \quad \text{and} \quad v(t, x) = \mathbb{E}[\mathcal{V}(x + W_{T-t} \sqrt{2\alpha})]. \quad (40)$$

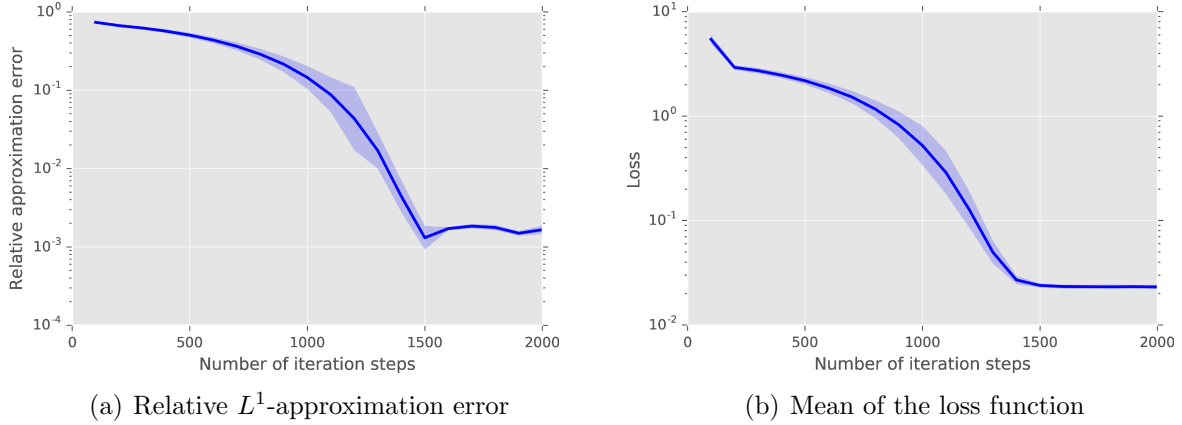


Figure 3: Relative L^1 -approximation error of \mathcal{U}^{Θ_m} and mean of the loss function against $m \in \{1, 2, 3, \dots, 2000\}$. The deep BSDE approximation $\mathcal{U}^{\Theta_{2000}} \approx u(0, \xi)$ achieves a relative L^1 -approximation error of size 0.0017 in a runtime of 283 seconds.

Observe that the hypothesis that $\sup_{x \in \mathbb{R}^d} [\beta g(x)] < \infty$ ensures that for all $\omega \in \Omega$ it holds that

$$\begin{aligned} \sup_{t \in [0, T]} \sup_{x \in \mathbb{R}^d} |\mathcal{V}(x + W_{T-t}(\omega) \sqrt{2\alpha})| &\leq \sup_{x \in \mathbb{R}^d} |\mathcal{V}(x)| = \sup_{x \in \mathbb{R}^d} \mathcal{V}(x) \\ &= \exp\left(\frac{\sup_{x \in \mathbb{R}^d} [\beta g(x)]}{\alpha}\right) < \infty. \end{aligned} \quad (41)$$

Combining this with Lebesgue's theorem of dominated convergence ensures that $v : [0, T] \times \mathbb{R}^d \rightarrow (0, \infty)$ is a continuous function. This and the fact that

$$\forall (t, x) \in [0, T] \times \mathbb{R}^d: u(t, x) = c \ln(v(t, x)) \quad (42)$$

establish Item (i). Next note that the Feynman-Kac formula ensures that for all $t \in [0, T]$, $x \in \mathbb{R}^d$ it holds that $v|_{[0, T] \times \mathbb{R}^d} \in C^{1,2}([0, T] \times \mathbb{R}^d, (0, \infty))$ and

$$\frac{\partial v}{\partial t}(t, x) + \alpha(\Delta_x v)(t, x) = 0. \quad (43)$$

This and (42) demonstrate Item (ii). It thus remains to prove Item (iii). For this note that the chain rule and (42) imply that for all $t \in [0, T]$, $x = (x_1, \dots, x_d) \in \mathbb{R}^d$, $i \in \{1, 2, \dots, d\}$ it holds that

$$\frac{\partial u}{\partial t}(t, x) = \frac{c}{v(t, x)} \cdot \frac{\partial v}{\partial t}(t, x) \quad \text{and} \quad \frac{\partial u}{\partial x_i}(t, x) = \frac{c}{v(t, x)} \cdot \frac{\partial v}{\partial x_i}(t, x). \quad (44)$$

Again the chain rule and (42) hence ensure that for all $t \in [0, T)$, $x = (x_1, \dots, x_d) \in \mathbb{R}^d$, $i \in \{1, 2, \dots, d\}$ it holds that

$$\frac{\partial u^2}{\partial x_i^2}(t, x) = \frac{c}{v(t, x)} \cdot \frac{\partial v^2}{\partial x_i^2}(t, x) - \frac{c}{[v(t, x)]^2} \cdot \left[\frac{\partial v}{\partial x_i}(t, x) \right]^2. \quad (45)$$

This assures that for all $t \in [0, T)$, $x = (x_1, \dots, x_d) \in \mathbb{R}^d$, $i \in \{1, 2, \dots, d\}$ it holds that

$$\begin{aligned} \alpha(\Delta_x u)(t, x) &= \frac{\alpha c}{v(t, x)} \cdot (\Delta_x v)(t, x) - \frac{\alpha c}{[v(t, x)]^2} \cdot \sum_{i=1}^d \left[\frac{\partial v}{\partial x_i}(t, x) \right]^2 \\ &= \frac{\alpha c(\Delta_x v)(t, x)}{v(t, x)} - \frac{\alpha c \|\nabla_x v(t, x)\|_{\mathbb{R}^d}^2}{[v(t, x)]^2}. \end{aligned} \quad (46)$$

Combining this with (44) demonstrates that for all $t \in [0, T)$, $x \in \mathbb{R}^d$ it holds that

$$\begin{aligned} \frac{\partial u}{\partial t}(t, x) + \alpha(\Delta_x u)(t, x) + \beta \|\nabla_x u(t, x)\|_{\mathbb{R}^d}^2 \\ = \frac{c}{v(t, x)} \cdot \frac{\partial v}{\partial t}(t, x) + \frac{\alpha c(\Delta_x v)(t, x)}{v(t, x)} - \frac{\alpha c \|\nabla_x v(t, x)\|_{\mathbb{R}^d}^2}{[v(t, x)]^2} + \beta \|\nabla_x u(t, x)\|_{\mathbb{R}^d}^2. \end{aligned} \quad (47)$$

Equation (43) hence shows that for all $t \in [0, T)$, $x = (x_1, \dots, x_d) \in \mathbb{R}^d$ it holds that

$$\begin{aligned} \frac{\partial u}{\partial t}(t, x) + \alpha(\Delta_x u)(t, x) + \beta \|\nabla_x u(t, x)\|_{\mathbb{R}^d}^2 \\ = \beta \|\nabla_x u(t, x)\|_{\mathbb{R}^d}^2 - \frac{\alpha c \|\nabla_x v(t, x)\|_{\mathbb{R}^d}^2}{[v(t, x)]^2} \\ = \beta \left[\sum_{i=1}^d \left| \frac{\partial u}{\partial x_i}(t, x) \right|^2 \right] - \frac{\alpha c \|\nabla_x v(t, x)\|_{\mathbb{R}^d}^2}{[v(t, x)]^2}. \end{aligned} \quad (48)$$

This and (44) demonstrate that for all $t \in [0, T)$, $x = (x_1, \dots, x_d) \in \mathbb{R}^d$ it holds that

$$\begin{aligned} \frac{\partial u}{\partial t}(t, x) + \alpha(\Delta_x u)(t, x) + \beta \|\nabla_x u(t, x)\|_{\mathbb{R}^d}^2 \\ = \beta \left[\sum_{i=1}^d \left| \frac{c}{v(t, x)} \cdot \frac{\partial v}{\partial x_i}(t, x) \right|^2 \right] - \frac{\alpha c \|\nabla_x v(t, x)\|_{\mathbb{R}^d}^2}{[v(t, x)]^2} \\ = \frac{c^2 \beta}{[v(t, x)]^2} \left[\sum_{i=1}^d \left| \frac{\partial v}{\partial x_i}(t, x) \right|^2 \right] - \frac{\alpha c \|\nabla_x v(t, x)\|_{\mathbb{R}^d}^2}{[v(t, x)]^2} \\ = \frac{[c^2 \beta - \alpha c] \|\nabla_x v(t, x)\|_{\mathbb{R}^d}^2}{[v(t, x)]^2} = 0. \end{aligned} \quad (49)$$

This and the fact that

$$\forall x \in \mathbb{R}^d: u(T, x) = c \ln(v(T, x)) = c \ln(\mathcal{V}(x)) = c \ln\left(\exp\left(\frac{g(x)}{c}\right)\right) = g(x) \quad (50)$$

establish Item (iii). The proof of Lemma 4.2 is thus completed. \square

4.4 Pricing of European financial derivatives with different interest rates for borrowing and lending

In this subsection we apply the deep BSDE solver to a pricing problem of an European financial derivative in a financial market where the risk free bank account used for the hedging of the financial derivative has different interest rates for borrowing and lending (see Bergman [4] and, e.g., [12, 2, 3, 5, 8, 11] where this example has been used as a test example for numerical methods for BSDEs).

Assume the setting in Subsection 4.1, let $\bar{\mu} = \frac{6}{100}$, $\bar{\sigma} = \frac{2}{10}$, $R^l = \frac{4}{100}$, $R^b = \frac{6}{100}$, and assume for all $s, t \in [0, T]$, $x = (x_1, \dots, x_d)$, $w = (w_1, \dots, w_d) \in \mathbb{R}^d$, $y \in \mathbb{R}$, $z \in \mathbb{R}^{1 \times d}$, $m \in \mathbb{N}$ that $d = 100$, $T = 1/2$, $N = 20$, $\gamma_m = 5 \cdot 10^{-3} = 0.005$, $\mu(t, x) = \bar{\mu}x$, $\sigma(t, x) = \bar{\sigma} \text{diag}_{\mathbb{R}^d \times d}(x_1, \dots, x_d)$, $\xi = (100, 100, \dots, 100) \in \mathbb{R}^d$, and

$$g(x) = \max\left\{\left[\max_{1 \leq i \leq 100} x_i\right] - 120, 0\right\} - 2 \max\left\{\left[\max_{1 \leq i \leq 100} x_i\right] - 150, 0\right\}, \quad (51)$$

$$\Upsilon(s, t, x, w) = \exp\left(\left(\bar{\mu} - \frac{\bar{\sigma}^2}{2}\right)(t - s)\right) \exp(\bar{\sigma} \text{diag}_{\mathbb{R}^d \times d}(w_1, \dots, w_d)) x, \quad (52)$$

$$f(t, x, y, z) = -R^l y - \frac{(\bar{\mu} - R^l)}{\bar{\sigma}} \sum_{i=1}^d z_i + (R^b - R^l) \max\left\{0, \left[\frac{1}{\bar{\sigma}} \sum_{i=1}^d z_i\right] - y\right\}. \quad (53)$$

Note that the solution u of the PDE (30) then satisfies for all $t \in [0, T]$, $x = (x_1, x_2, \dots, x_d) \in \mathbb{R}^d$ that $u(T, x) = g(x)$ and

$$\begin{aligned} \frac{\partial u}{\partial t}(t, x) + f(t, x, u(t, x), \bar{\sigma} \text{diag}_{\mathbb{R}^d \times d}(x_1, \dots, x_d)(\nabla_x u)(t, x)) + \bar{\mu} \sum_{i=1}^d x_i \frac{\partial u}{\partial x_i}(t, x) \\ + \frac{\bar{\sigma}^2}{2} \sum_{i=1}^d |x_i|^2 \frac{\partial^2 u}{\partial x_i^2}(t, x) = 0. \end{aligned} \quad (54)$$

Hence, we obtain for all $t \in [0, T]$, $x = (x_1, x_2, \dots, x_d) \in \mathbb{R}^d$ that $u(T, x) = g(x)$ and

$$\begin{aligned} \frac{\partial u}{\partial t}(t, x) + \frac{\bar{\sigma}^2}{2} \sum_{i=1}^d |x_i|^2 \frac{\partial^2 u}{\partial x_i^2}(t, x) \\ + \max\left\{R^b \left(\left[\sum_{i=1}^d x_i \left(\frac{\partial u}{\partial x_i}\right)(t, x)\right] - u(t, x)\right), R^l \left(\left[\sum_{i=1}^d x_i \left(\frac{\partial u}{\partial x_i}\right)(t, x)\right] - u(t, x)\right)\right\} = 0. \end{aligned} \quad (55)$$

This shows that for all $t \in [0, T)$, $x = (x_1, x_2, \dots, x_d) \in \mathbb{R}^d$ it holds that $u(T, x) = g(x)$ and

$$\frac{\partial u}{\partial t}(t, x) + \frac{\bar{\sigma}^2}{2} \sum_{i=1}^d |x_i|^2 \frac{\partial^2 u}{\partial x_i^2}(t, x) - \min \left\{ R^b \left(u(t, x) - \sum_{i=1}^d x_i \frac{\partial u}{\partial x_i}(t, x) \right), R^l \left(u(t, x) - \sum_{i=1}^d x_i \frac{\partial u}{\partial x_i}(t, x) \right) \right\} = 0. \quad (56)$$

In Table 3 we approximatively calculate the mean of \mathcal{U}^{Θ_m} , the standard deviation of \mathcal{U}^{Θ_m} , the relative L^1 -approximatin error associated to \mathcal{U}^{Θ_m} , the standard deviation of the relative L^1 -approximatin error associated to \mathcal{U}^{Θ_m} , and the runtime in seconds needed to calculate one realization of \mathcal{U}^{Θ_m} against $m \in \{0, 1000, 2000, 3000, 4000\}$ based on 5 independent realizations (5 independent runs). Table 3 also depicts the mean of the loss function associated to Θ_m and the standard deviation of the loss function associated to Θ_m against $m \in \{0, 1000, 2000, 3000, 4000\}$ based on 256 Monte Carlo samples and 5 independent realizations (5 independent runs). In addition, the relative L^1 -approximation error associated to \mathcal{U}^{Θ_m} against $m \in \{1, 2, 3, \dots, 4000\}$ is pictured on the left hand side of Figure 4 based on 5 independent realizations (5 independent runs) and the mean of the loss function associated to Θ_m against $m \in \{1, 2, 3, \dots, 4000\}$ is pictured on the right hand side of Figure 4 based on 256 Monte Carlo samples and 5 independent realizations (5 independent runs). In the approximative computations of the relative L^1 -approximation errors in Table 3 and Figure 4 the value $u(0, \xi) = u(0, 0, \dots, 0)$ of the exact solution u of the PDE (56) is replaced by the value 21.299 which, in turn, is calculated by means of the multilevel-Picard approximation method in E et al. [11] (see [11, $\rho = 7$ in Table 6 in Section 4.3]).

Number of iteration steps m	Mean of \mathcal{U}^{Θ_m}	Standard deviation of \mathcal{U}^{Θ_m}	Relative L^1 -appr. error	Standard deviation of the relative L^1 -appr. error	Mean of the loss function	Standard deviation of the loss function	Runtime in sec. for one realization of \mathcal{U}^{Θ_m}
0	16.964	0.882	0.204	0.041	53.666	8.957	
1000	20.309	0.524	0.046	0.025	30.886	3.076	194
2000	21.150	0.098	0.007	0.005	29.197	3.160	331
3000	21.229	0.034	0.003	0.002	29.070	3.246	470
4000	21.217	0.043	0.004	0.002	29.029	3.236	617

Table 3: Numerical simulations for the deep BSDE solver in Subsection 3.2 in the case of the PDE (56).

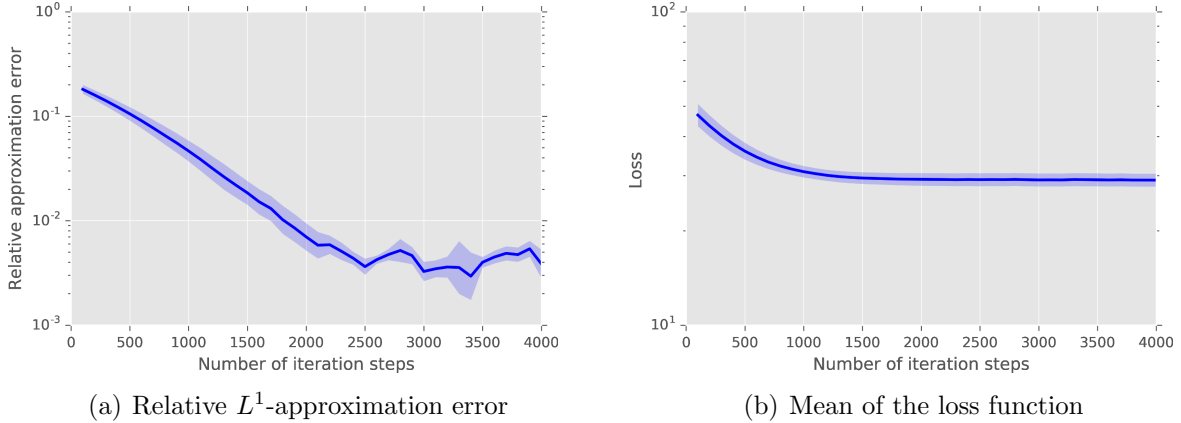


Figure 4: Relative L^1 -approximation error of \mathcal{U}^{Θ_m} and mean of the loss function against $m \in \{1, 2, 3, \dots, 4000\}$ in the case of the PDE (56). The deep BSDE approximation $\mathcal{U}^{\Theta_{4000}} \approx u(0, \xi)$ achieves a relative L^1 -approximation error of size 0.0039 in a runtime of 566 seconds.

4.5 Multidimensional Burgers-type PDEs with explicit solutions

In this subsection we consider a high-dimensional version of the example analyzed numerically in Chassagneux [6, Example 4.6 in Subsection 4.2].

More specifically, assume the setting in Subsection 4.1, and assume for all $s, t \in [0, T]$, $x = (x_1, \dots, x_d), w = (w_1, \dots, w_d) \in \mathbb{R}^d$, $y \in \mathbb{R}$, $z = (z_i)_{i \in \{1, 2, \dots, d\}} \in \mathbb{R}^{1 \times d}$ that $\mu(t, x) = 0$, $\sigma(t, x)w = \frac{d}{\sqrt{2}}w$, $\xi = (0, 0, \dots, 0) \in \mathbb{R}^d$, $\Upsilon(s, t, x, w) = x + \frac{d}{\sqrt{2}}w$, and

$$g(x) = \frac{\exp(T + \frac{1}{d} \sum_{i=1}^d x_i)}{(1 + \exp(T + \frac{1}{d} \sum_{i=1}^d x_i))}, \quad f(t, x, y, z) = \left(y - \frac{2+d}{2d}\right) \left(\sum_{i=1}^d z_i\right). \quad (57)$$

Note that the solution u of the PDE (30) then satisfies for all $t \in [0, T)$, $x = (x_1, x_2, \dots, x_d) \in \mathbb{R}^d$ that $u(T, x) = g(x)$ and

$$\frac{\partial u}{\partial t}(t, x) + \frac{d^2}{2}(\Delta_x u)(t, x) + \left(u(t, x) - \frac{2+d}{2d}\right) \left(d \sum_{i=1}^d \frac{\partial u}{\partial x_i}(t, x)\right) = 0 \quad (58)$$

(cf. Lemma 4.3 below [with $\alpha = d^2$, $\kappa = 1/d$ in the notation of Lemma 4.3 below]). On the left hand side of Figure 5 we present approximatively the relative L^1 -approximation error associated to \mathcal{U}^{Θ_m} against $m \in \{1, 2, 3, \dots, 60\,000\}$ based on 5 independent realizations (5 independent runs) in the case

$$T = 1, \quad d = 20, \quad N = 80, \quad \forall m \in \mathbb{N}: \gamma_m = 10^{(\mathbb{1}_{[1, 30000]}(m) + \mathbb{1}_{[1, 50000]}(m) - 4)}. \quad (59)$$

On the right hand side of Figure 5 we present approximately the mean of the loss function associated to Θ_m against $m \in \{1, 2, 3, \dots, 60\,000\}$ based on 256 Monte Carlo samples and 5 independent realizations (5 independent runs) in the case (59). On the left hand side of Figure 6 we present approximately the relative L^1 -approximation error associated to \mathcal{U}^{Θ_m} against $m \in \{1, 2, 3, \dots, 30\,000\}$ based on 5 independent realizations (5 independent runs) in the case

$$T = \frac{2}{10}, \quad d = 50, \quad N = 30, \quad \forall m \in \mathbb{N}: \gamma_m = 10^{(\mathbb{1}_{[1,15000]}(m) + \mathbb{1}_{[1,25000]}(m) - 4)}. \quad (60)$$

On the right hand side of Figure 6 we present approximately the mean of the loss function associated to Θ_m against $m \in \{1, 2, 3, \dots, 30\,000\}$ based on 256 Monte Carlo samples and 5 independent realizations (5 independent runs) in the case (60).

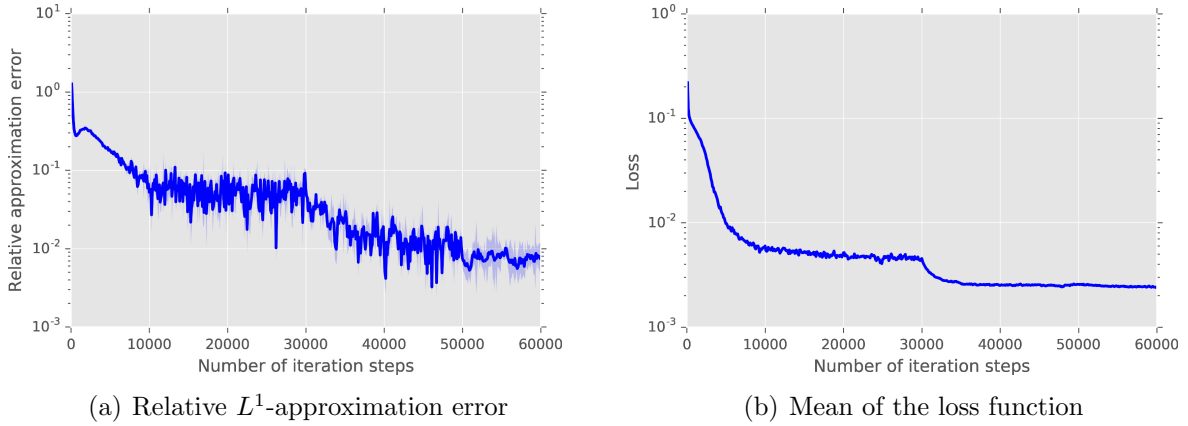


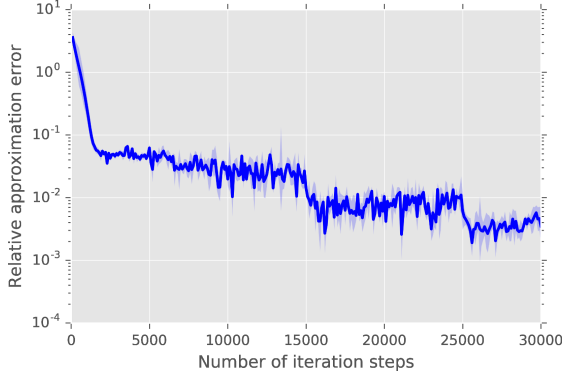
Figure 5: Relative L^1 -approximation error of \mathcal{U}^{Θ_m} and mean of the loss function against $m \in \{1, 2, 3, \dots, 60\,000\}$ in the case of the PDE (58) with (59). The deep BSDE approximation $\mathcal{U}^{\Theta_{60\,000}} \approx u(0, \xi)$ achieves a relative L^1 -approximation error of size 0.0073 in a runtime of 20 389 seconds.

Lemma 4.3 (Cf. Example 4.6 in Subsection 4.2 in [6]). *Let $\alpha, \kappa, T \in (0, \infty)$, $d \in \mathbb{N}$, let $u: [0, T] \times \mathbb{R}^d \rightarrow \mathbb{R}$ be the function which satisfies for all $t \in [0, T]$, $x = (x_1, \dots, x_d) \in \mathbb{R}^d$ that*

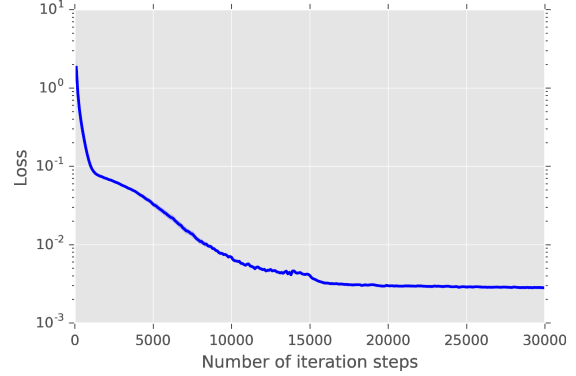
$$u(t, x) = 1 - \frac{1}{(1 + \exp(t + \kappa \sum_{i=1}^d x_i))} = \frac{\exp(t + \kappa \sum_{i=1}^d x_i)}{(1 + \exp(t + \kappa \sum_{i=1}^d x_i))}, \quad (61)$$

and let $f: [0, T] \times \mathbb{R}^d \times \mathbb{R}^{1+d} \rightarrow \mathbb{R}$ be the function which satisfies for all $t \in [0, T]$, $x \in \mathbb{R}^d$, $y \in \mathbb{R}$, $z = (z_1, \dots, z_d) \in \mathbb{R}^d$ that

$$f(t, x, y, z) = \left(\alpha \kappa y - \frac{1}{d \kappa} - \frac{\alpha \kappa}{2} \right) \left(\sum_{i=1}^d z_i \right). \quad (62)$$



(a) Relative L^1 -approximation error



(b) Mean of the loss function

Figure 6: Relative L^1 -approximation error of \mathcal{U}^{Θ_m} and mean of the loss function against $m \in \{1, 2, 3, \dots, 30\,000\}$ in the case of the PDE (58) with (60). The deep BSDE approximation $\mathcal{U}^{\Theta_{30\,000}} \approx u(0, \xi)$ achieves a relative L^1 -approximation error of size 0.0035 in a runtime of 4281 seconds.

Then it holds for all $t \in [0, T]$, $x \in \mathbb{R}^d$ that

$$\frac{\partial u}{\partial t}(t, x) + \frac{\alpha}{2}(\Delta_x u)(t, x) + f(t, x, u(t, x), (\nabla_x u)(t, x)) = 0. \quad (63)$$

Proof of Lemma 4.3. Throughout this proof let $\beta, \gamma \in (0, \infty)$ be the real numbers given by

$$\beta = \alpha\kappa \quad \text{and} \quad \gamma = \frac{1}{d\kappa} + \frac{\alpha\kappa}{2} \quad (64)$$

and let $w: [0, T] \times \mathbb{R}^d \rightarrow (0, \infty)$ be the function which satisfies for all $t \in [0, T]$, $x = (x_1, \dots, x_d) \in \mathbb{R}^d$ that

$$w(t, x) = \exp\left(t + \kappa \sum_{i=1}^d x_i\right). \quad (65)$$

Observe that for all $t \in [0, T]$, $x = (x_1, \dots, x_d) \in \mathbb{R}^d$, $i \in \{1, 2, \dots, d\}$ it holds that

$$u(t, x) = 1 - [1 + w(t, x)]^{-1} = \frac{[1 + w(t, x)]}{[1 + w(t, x)]} - \frac{1}{[1 + w(t, x)]} = \frac{w(t, x)}{1 + w(t, x)}, \quad (66)$$

$$\frac{\partial u}{\partial t}(t, x) = [1 + w(t, x)]^{-2} \cdot \frac{\partial w}{\partial t}(t, x) = \frac{w(t, x)}{[1 + w(t, x)]^2}, \quad (67)$$

and

$$\frac{\partial u}{\partial x_i}(t, x) = [1 + w(t, x)]^{-2} \cdot \frac{\partial w}{\partial x_i}(t, x) = \kappa w(t, x) [1 + w(t, x)]^{-2}. \quad (68)$$

Note that (66), (67), and (68) ensure that for all $t \in [0, T]$, $x \in \mathbb{R}^d$ it holds that

$$\begin{aligned}
& \frac{\partial u}{\partial t}(t, x) + \frac{\alpha}{2}(\Delta_x u)(t, x) + f(t, x, u(t, x), (\nabla_x u)(t, x)) \\
&= \frac{\partial u}{\partial t}(t, x) + \frac{\alpha}{2}(\Delta_x u)(t, x) + (\beta u(t, x) - \gamma) \left(\sum_{i=1}^d \frac{\partial u}{\partial x_i}(t, x) \right) \\
&= \frac{\partial u}{\partial t}(t, x) + \frac{\alpha}{2}(\Delta_x u)(t, x) + d \frac{\partial u}{\partial x_1}(t, x) (\beta u(t, x) - \gamma) \\
&= \frac{w(t, x)}{[1 + w(t, x)]^2} + \frac{\alpha}{2}(\Delta_x u)(t, x) + \frac{d\kappa w(t, x)}{[1 + w(t, x)]^2} \left(\frac{\beta w(t, x)}{[1 + w(t, x)]} - \gamma \right).
\end{aligned} \tag{69}$$

Moreover, observe that (68) demonstrates that for all $t \in [0, T]$, $x \in \mathbb{R}^d$ it holds that

$$\begin{aligned}
\frac{\partial^2 u}{\partial x_i^2}(t, x) &= \kappa \frac{\partial w}{\partial x_i}(t, x) [1 + w(t, x)]^{-2} - 2\kappa w(t, x) [1 + w(t, x)]^{-3} \frac{\partial w}{\partial x_i}(t, x) \\
&= \frac{\kappa^2 w(t, x)}{[1 + w(t, x)]^2} - \frac{2\kappa^2 |w(t, x)|^2}{[1 + w(t, x)]^3} = \frac{\kappa^2 w(t, x)}{[1 + w(t, x)]^2} \left[1 - \frac{2w(t, x)}{[1 + w(t, x)]} \right].
\end{aligned} \tag{70}$$

Hence, we obtain that for all $t \in [0, T]$, $x \in \mathbb{R}^d$ it holds that

$$\frac{\alpha}{2}(\Delta_x u)(t, x) = \frac{d\alpha}{2} \frac{\partial^2 u}{\partial x_1^2}(t, x) = \frac{d\alpha\kappa^2 w(t, x)}{2[1 + w(t, x)]^2} \left[1 - \frac{2w(t, x)}{[1 + w(t, x)]} \right]. \tag{71}$$

Combining this with (69) implies that for all $t \in [0, T]$, $x \in \mathbb{R}^d$ it holds that

$$\begin{aligned}
& \frac{\partial u}{\partial t}(t, x) + \frac{\alpha}{2}(\Delta_x u)(t, x) + f(t, x, u(t, x), (\nabla_x u)(t, x)) \\
&= \frac{w(t, x) [1 - d\kappa\gamma]}{[1 + w(t, x)]^2} + \frac{\alpha}{2}(\Delta_x u)(t, x) + \frac{d\beta\kappa |w(t, x)|^2}{[1 + w(t, x)]^3} \\
&= \frac{w(t, x) [1 - d\kappa\gamma]}{[1 + w(t, x)]^2} + \frac{d\alpha\kappa^2 w(t, x)}{2[1 + w(t, x)]^2} \left[1 - \frac{2w(t, x)}{[1 + w(t, x)]} \right] + \frac{d\beta\kappa |w(t, x)|^2}{[1 + w(t, x)]^3} \\
&= \frac{w(t, x) [1 - d\kappa\gamma + \frac{d\alpha\kappa^2}{2}]}{[1 + w(t, x)]^2} - \frac{d\alpha\kappa^2 |w(t, x)|^2}{[1 + w(t, x)]^3} + \frac{d\beta\kappa |w(t, x)|^2}{[1 + w(t, x)]^3}.
\end{aligned} \tag{72}$$

The fact that $\alpha\kappa^2 = \beta\kappa$ hence demonstrates that for all $t \in [0, T]$, $x \in \mathbb{R}^d$ it holds that

$$\begin{aligned}
& \frac{\partial u}{\partial t}(t, x) + \frac{\alpha}{2}(\Delta_x u)(t, x) + f(t, x, u(t, x), (\nabla_x u)(t, x)) \\
&= \frac{w(t, x) [1 - d\kappa\gamma + \frac{d\alpha\kappa^2}{2}]}{[1 + w(t, x)]^2}.
\end{aligned} \tag{73}$$

This and the fact that $1 + \frac{d\alpha\kappa^2}{2} = d\kappa\gamma$ show that for all $t \in [0, T]$, $x \in \mathbb{R}^d$ it holds that

$$\frac{\partial u}{\partial t}(t, x) + \frac{\alpha}{2}(\Delta_x u)(t, x) + f(t, x, u(t, x), (\nabla_x u)(t, x)) = 0. \quad (74)$$

The proof of Lemma 4.3 is thus completed. \square

4.6 An example PDE with quadratically growing derivatives and an explicit solution

In this subsection we consider a high-dimensional version of the example analyzed numerically in Gobet & Turkedjiev [13, Section 5]. More specifically, Gobet & Turkedjiev [13, Section 5] employ the PDE in (76) below as a numerical test example but with the time horizon $T = 2/10$ instead of $T = 1$ in this article and with the dimension $d \in \{3, 5, 7\}$ instead of $d = 100$ in this article.

Assume the setting in Subsection 4.1, let $\alpha = 4/10$, let $\psi: [0, T] \times \mathbb{R}^d \rightarrow \mathbb{R}$ be the function which satisfies for all $(t, x) \in [0, T] \times \mathbb{R}^d$ that $\psi(t, x) = \sin([T - t + \|x\|_{\mathbb{R}^d}^2]^\alpha)$, and assume for all $s \in [0, T]$, $t \in [0, T]$, $x, w \in \mathbb{R}^d$, $y \in \mathbb{R}$, $z \in \mathbb{R}^{1 \times d}$, $m \in \mathbb{N}$ that $T = 1$, $d = 100$, $N = 30$, $\gamma_m = 5 \cdot 10^{-3} = \frac{5}{1000} = 0.005$, $\mu(t, x) = 0$, $\sigma(t, x)w = w$, $\xi = (0, 0, \dots, 0) \in \mathbb{R}^d$, $\Upsilon(t, s, x, w) = x + w$, $g(x) = \sin(\|x\|_{\mathbb{R}^d}^{2\alpha})$, and

$$f(t, x, y, z) = \|z\|_{\mathbb{R}^{1 \times d}}^2 - \|(\nabla_x \psi)(t, x)\|_{\mathbb{R}^d}^2 - \frac{\partial \psi}{\partial t}(t, x) - \frac{1}{2}(\Delta_x \psi)(t, x). \quad (75)$$

Note that the solution u of the PDE (30) then satisfies for all $t \in [0, T]$, $x = (x_1, x_2, \dots, x_d) \in \mathbb{R}^d$ that $u(T, x) = g(x)$ and

$$\frac{\partial u}{\partial t}(t, x) + \|(\nabla_x u)(t, x)\|_{\mathbb{R}^d}^2 + \frac{1}{2}(\Delta_x u)(t, x) = \frac{\partial \psi}{\partial t}(t, x) + \|(\nabla_x \psi)(t, x)\|_{\mathbb{R}^d}^2 + \frac{1}{2}(\Delta_x \psi)(t, x). \quad (76)$$

On the left hand side of Figure 7 we present approximately the relative L^1 -approximation error associated to \mathcal{U}^{Θ_m} against $m \in \{1, 2, 3, \dots, 4000\}$ based on 5 independent realizations (5 independent runs). On the right hand side of Figure 7 we present approximately the mean of the loss function associated to Θ_m against $m \in \{1, 2, 3, \dots, 4000\}$ based on 256 Monte Carlo samples and 5 independent realizations (5 independent runs).

4.7 Time-dependent reaction-diffusion-type example PDEs with oscillating explicit solutions

In this subsection we consider a high-dimensional version of the example PDE analyzed numerically in Gobet & Turkedjiev [14, Subsection 6.1]. More specifically, Gobet & Turkedjiev [14, Subsection 6.1] employ the PDE in (78) below as a numerical test example

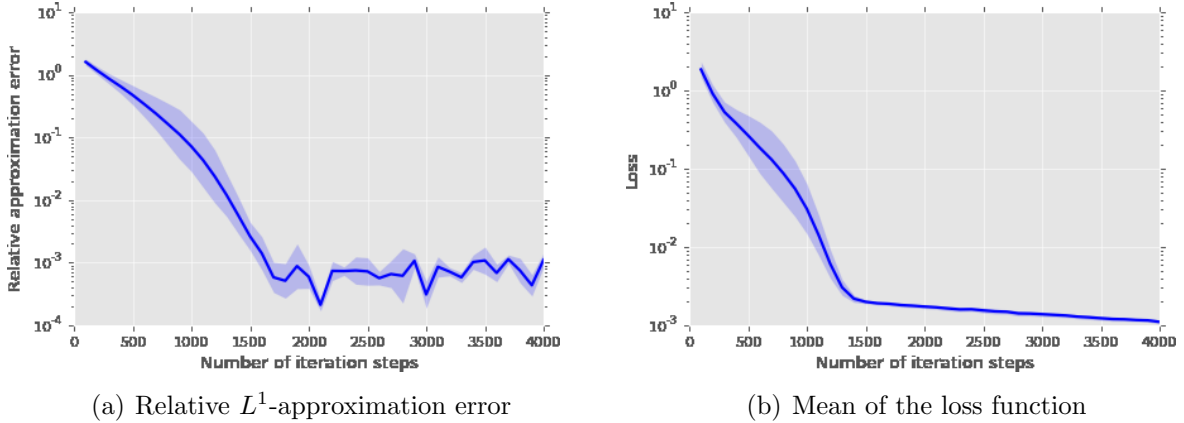


Figure 7: Relative L^1 -approximation error of \mathcal{U}^{Θ_m} and mean of the loss function against $m \in \{1, 2, 3, \dots, 4000\}$ in the case of the PDE (76). The deep BSDE approximation $\mathcal{U}^{\Theta_{4000}} \approx u(0, \xi)$ achieves a relative L^1 -approximation error of size 0.0009 in a runtime of 957 seconds.

but in two space-dimensions ($d = 2$) instead of in hundred space-dimensions ($d = 100$) as in this article.

Assume the setting in Subsection 4.1, let $\kappa = 6/10$, $\lambda = 1/\sqrt{d}$, assume for all $s, t \in [0, T]$, $x = (x_1, \dots, x_d), w = (w_1, \dots, w_d) \in \mathbb{R}^d$, $y \in \mathbb{R}$, $z \in \mathbb{R}^{1 \times d}$, $m \in \mathbb{N}$ that $\gamma_m = \frac{1}{100} = 0.01$, $T = 1$, $d = 100$, $N = 30$, $\mu(t, x) = 0$, $\sigma(t, x)w = w$, $\xi = (0, 0, \dots, 0) \in \mathbb{R}^d$, $\Upsilon(s, t, x, w) = x + w$, $g(x) = 1 + \kappa + \sin(\lambda \sum_{i=1}^d x_i)$, and

$$f(t, x, y, z) = \min \left\{ 1, \left[y - \kappa - 1 - \sin(\lambda \sum_{i=1}^d x_i) \exp\left(\frac{\lambda^2 d(t-T)}{2}\right) \right]^2 \right\}. \quad (77)$$

Note that the solution u of the PDE (30) then satisfies for all $t \in [0, T]$, $x = (x_1, x_2, \dots, x_d) \in \mathbb{R}^d$ that $u(T, x) = g(x)$ and

$$\frac{\partial u}{\partial t}(t, x) + \min \left\{ 1, \left[u(t, x) - \kappa - 1 - \sin(\lambda \sum_{i=1}^d x_i) \exp\left(\frac{\lambda^2 d(t-T)}{2}\right) \right]^2 \right\} + \frac{1}{2} (\Delta_x u)(t, x) = 0 \quad (78)$$

(cf. Lemma 4.4 below). On the left hand side of Figure 7 we present approximatively the relative L^1 -approximation error associated to \mathcal{U}^{Θ_m} against $m \in \{1, 2, 3, \dots, 24000\}$ based on 5 independent realizations (5 independent runs). On the right hand side of Figure 7 we present approximatively the mean of the loss function associated to Θ_m against $m \in \{1, 2, 3, \dots, 24000\}$ based on 256 Monte Carlo samples and 5 independent realizations (5 independent runs).

Lemma 4.4 (Cf. Subsection 6.1 in [14]). *Let $T, \kappa, \lambda \in (0, \infty)$, $d \in \mathbb{N}$ and let $u: [0, T] \times \mathbb{R}^d \rightarrow \mathbb{R}$ be the function which satisfies for all $t \in [0, T]$, $x = (x_1, \dots, x_d) \in \mathbb{R}^d$ that*

$$u(t, x) = 1 + \kappa + \sin\left(\lambda \sum_{i=1}^d x_i\right) \exp\left(\frac{\lambda^2 d(t-T)}{2}\right). \quad (79)$$

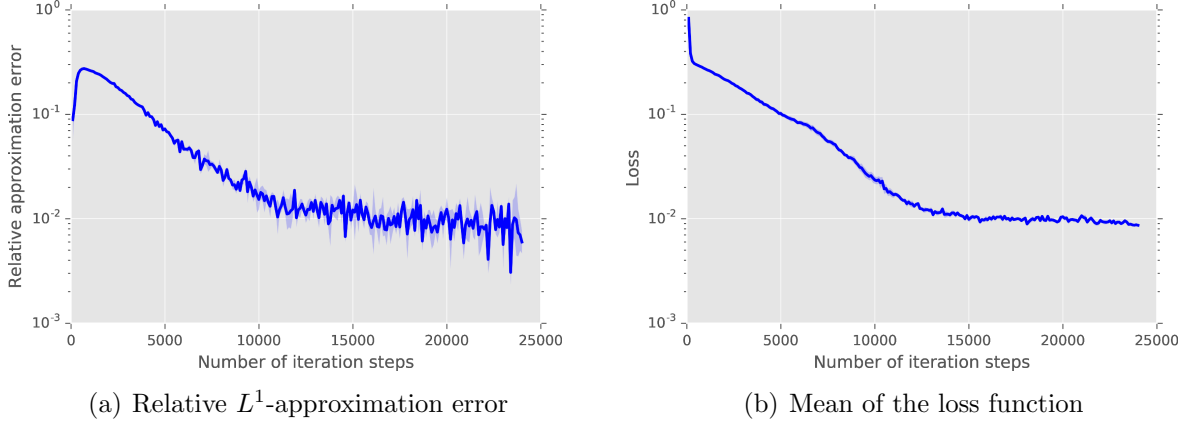


Figure 8: Relative L^1 -approximation error of \mathcal{U}^{Θ_m} and mean of the loss function against $m \in \{1, 2, 3, \dots, 24000\}$ in the case of the PDE (78). The deep BSDE approximation $\mathcal{U}^{\Theta_{24000}} \approx u(0, \xi)$ achieves a relative L^1 -approximation error of size 0.0060 in a runtime of 4872 seconds.

Then it holds for all $t \in [0, T]$, $x = (x_1, \dots, x_d) \in \mathbb{R}^d$ that $u \in C^{1,2}([0, T] \times \mathbb{R}^d, \mathbb{R})$, $u(T, x) = 1 + \kappa + \sin(\lambda \sum_{i=1}^d x_i)$, and

$$\frac{\partial u}{\partial t}(t, x) + \min\left\{1, [u(t, x) - \kappa - 1 - \sin(\lambda \sum_{i=1}^d x_i) \exp(\frac{\lambda^2 d(t-T)}{2})]^2\right\} + \frac{1}{2} (\Delta_x u)(t, x) = 0. \quad (80)$$

Proof of Lemma 4.4. Note that for all $t \in [0, T]$, $x = (x_1, \dots, x_d) \in \mathbb{R}^d$ it holds that

$$\frac{\partial u}{\partial t}(t, x) = \frac{\lambda^2 d}{2} \sin(\lambda \sum_{i=1}^d x_i) \exp(\frac{\lambda^2 d(t-T)}{2}). \quad (81)$$

In addition, observe that for all $t \in [0, T]$, $x = (x_1, \dots, x_d) \in \mathbb{R}^d$, $k \in \{1, 2, \dots, d\}$ it holds that

$$\frac{\partial u}{\partial x_k}(t, x) = \lambda \cos(\lambda \sum_{i=1}^d x_i) \exp(\frac{\lambda^2 d(t-T)}{2}). \quad (82)$$

Hence, we obtain that for all $t \in [0, T]$, $x = (x_1, \dots, x_d) \in \mathbb{R}^d$, $k \in \{1, \dots, d\}$ it holds that

$$\frac{\partial^2 u}{\partial x_k^2}(t, x) = -\lambda^2 \sin(\lambda \sum_{i=1}^d x_i) \exp(\frac{\lambda^2 d(t-T)}{2}). \quad (83)$$

This ensures that for all $t \in [0, T]$, $x = (x_1, \dots, x_d) \in \mathbb{R}^d$ it holds that

$$(\Delta_x u)(t, x) = -d \lambda^2 \sin(\lambda \sum_{i=1}^d x_i) \exp(\frac{\lambda^2 d(t-T)}{2}). \quad (84)$$

Combining this with (81) proves that for all $t \in [0, T]$, $x = (x_1, \dots, x_d) \in \mathbb{R}^d$ it holds that

$$\frac{\partial u}{\partial t}(t, x) + \frac{1}{2} (\Delta_x u)(t, x) = 0. \quad (85)$$

This demonstrates that for all $t \in [0, T]$, $x = (x_1, \dots, x_d) \in \mathbb{R}^d$ it holds that

$$\begin{aligned} & \frac{\partial v}{\partial t}(t, x) + \min \left\{ 1, [v(t, x) - \kappa - 1 - \sin(\lambda \sum_{i=1}^d x_i) \exp(\frac{\lambda^2 d(t-T)}{2})]^2 \right\} + \frac{1}{2} (\Delta_x v)(t, x) \\ &= \frac{\partial v}{\partial t}(t, x) + \frac{1}{2} (\Delta_x v)(t, x) = 0. \end{aligned} \quad (86)$$

The proof of Lemma 4.4 is thus completed. \square

5 Appendix A: Special cases of the proposed algorithm

In this subsection we illustrate the general algorithm in Subsection 3.2 in several special cases. More specifically, in Subsections 5.1 and 5.2 we provide special choices for the functions ψ_m , $m \in \mathbb{N}$, and Ψ_m , $m \in \mathbb{N}$, employed in (29) and in Subsections 5.3 and 5.4 we provide special choices for the function Υ in (24).

5.1 Stochastic gradient descent (SGD)

Example 5.1. Assume the setting in Subsection 3.2, let $(\gamma_m)_{m \in \mathbb{N}} \subseteq (0, \infty)$, and assume for all $m \in \mathbb{N}$, $x \in \mathbb{R}^e$, $(\varphi_j)_{j \in \mathbb{N}} \in (\mathbb{R}^\rho)^\mathbb{N}$ that

$$\varrho = \rho, \quad \Psi_m(x, (\varphi_j)_{j \in \mathbb{N}}) = \varphi_1, \quad \text{and} \quad \psi_m(x) = \gamma_m x. \quad (87)$$

Then it holds for all $m \in \mathbb{N}$ that

$$\Theta_m = \Theta_{m-1} - \gamma_m \Phi_{m-1,1}(\Theta_{m-1}). \quad (88)$$

5.2 Adaptive Moment Estimation (Adam) with mini-batches

In this subsection we illustrate how the so-called Adam optimizer (see [22]) can be employed in conjunction with the deep BSDE solver in Subsection 3.2 (cf. also Subsection 4.1 above).

Example 5.2. Assume the setting in Subsection 3.2, assume that $\varrho = 2\rho$, let $\text{Pow}_r: \mathbb{R}^\rho \rightarrow \mathbb{R}^\rho$, $r \in (0, \infty)$, be the functions which satisfy for all $r \in (0, \infty)$, $x = (x_1, \dots, x_\rho) \in \mathbb{R}^\rho$ that

$$\text{Pow}_r(x) = (|x_1|^r, \dots, |x_\rho|^r), \quad (89)$$

let $\varepsilon \in (0, \infty)$, $(\gamma_m)_{m \in \mathbb{N}} \subseteq (0, \infty)$, $(J_m)_{m \in \mathbb{N}_0} \subseteq \mathbb{N}$, $\mathbb{X}, \mathbb{Y} \in (0, 1)$, let $\mathbf{m}, \mathbb{M}: \mathbb{N}_0 \times \Omega \rightarrow \mathbb{R}^\rho$ be the stochastic processes which satisfy for all $m \in \mathbb{N}_0$ that $\Xi_m = (\mathbf{m}_m, \mathbb{M}_m)$, and assume for all $m \in \mathbb{N}$, $x, y \in \mathbb{R}^\rho$, $(\varphi_j)_{j \in \mathbb{N}} \in (\mathbb{R}^\rho)^\mathbb{N}$ that

$$\Psi_m(x, y, (\varphi_j)_{j \in \mathbb{N}}) = (\mathbb{X}x + (1 - \mathbb{X})\left(\frac{1}{J_m} \sum_{j=1}^{J_m} \varphi_j\right), \mathbb{Y}y + (1 - \mathbb{Y})\text{Pow}_2\left(\frac{1}{J_m} \sum_{j=1}^{J_m} \varphi_j\right)) \quad (90)$$

and

$$\psi_m(x, y) = \left[\varepsilon + \text{Pow}_{1/2}\left(\frac{y}{(1 - \mathbb{Y}^m)}\right) \right]^{-1} \frac{\gamma_m x}{(1 - \mathbb{X}^m)}. \quad (91)$$

Then it holds for all $m \in \mathbb{N}$ that

$$\begin{aligned} \Theta_m &= \Theta_{m-1} - \left[\varepsilon + \text{Pow}_{1/2}\left(\frac{\mathbb{M}_m}{(1 - \mathbb{Y}^m)}\right) \right]^{-1} \frac{\gamma_m \mathbf{m}_m}{(1 - \mathbb{X}^m)}, \\ \mathbf{m}_m &= \mathbb{X} \mathbf{m}_{m-1} + \frac{(1 - \mathbb{X})}{J_m} \left(\sum_{j=1}^{J_m} \Phi_{\mathbb{S}_m}^{m-1, j}(\Theta_{m-1}) \right), \\ \mathbb{M}_m &= \mathbb{Y} \mathbb{M}_{m-1} + (1 - \mathbb{Y}) \text{Pow}_2\left(\frac{1}{J_m} \sum_{j=1}^{J_m} \Phi_{\mathbb{S}_m}^{m-1, j}(\Theta_{m-1})\right). \end{aligned} \quad (92)$$

5.3 Geometric Brownian motion

Example 5.3. Assume the setting in Section 3.2, let $\bar{\mu}, \bar{\sigma} \in \mathbb{R}$, and assume for all $s, t \in [0, T]$, $x = (x_1, \dots, x_d)$, $w = (w_1, \dots, w_d) \in \mathbb{R}^d$ that

$$\Upsilon(s, t, x, w) = \exp\left(\left(\bar{\mu} - \frac{\bar{\sigma}^2}{2}\right)(t - s)\right) \exp(\bar{\sigma} \text{diag}_{\mathbb{R}^d \times d}(w_1, \dots, w_d)) x. \quad (93)$$

Then it holds for all $m, j \in \mathbb{N}_0$, $n \in \{0, 1, \dots, N\}$ that

$$\mathcal{X}_n^{\theta, m, j} = \exp\left(\left(\bar{\mu} - \frac{\bar{\sigma}^2}{2}\right) t_n \text{Id}_{\mathbb{R}^d} + \bar{\sigma} \text{diag}_{\mathbb{R}^d \times d}(W_{t_n}^{m, j})\right) \xi. \quad (94)$$

In the setting of Example 5.3 we consider under suitable further hypotheses (cf. Subsection 4.4 above) for every sufficiently large $m \in \mathbb{N}_0$ the random variable \mathcal{U}^{Θ_m} as an approximation of $u(0, \xi)$ where $u: [0, T] \times \mathbb{R}^d \rightarrow \mathbb{R}^k$ is a suitable solution of the PDE

$$\begin{aligned} \frac{\partial u}{\partial t}(t, x) + \frac{\bar{\sigma}^2}{2} \sum_{i=1}^d |x_i|^2 \left(\frac{\partial^2 u}{\partial x_i^2}\right)(t, x) + \bar{\mu} \sum_{i=1}^d x_i \left(\frac{\partial u}{\partial x_i}\right)(t, x) \\ + f(t, x, u(t, x), \bar{\sigma} \left(\frac{\partial u}{\partial x}\right)(t, x) \text{diag}_{\mathbb{R}^d \times d}(x_1, \dots, x_d)) = 0 \end{aligned} \quad (95)$$

with $u(T, x) = g(x)$ for $t \in [0, T]$, $x = (x_1, \dots, x_d) \in \mathbb{R}^d$.

5.4 Euler-Maruyama scheme

Example 5.4. Assume the setting in Section 3.2, let $\mu: [0, T] \times \mathbb{R}^d \rightarrow \mathbb{R}^d$ and $\sigma: [0, T] \times \mathbb{R}^d \rightarrow \mathbb{R}^d$ be functions, and assume for all $s, t \in [0, T]$, $x, w \in \mathbb{R}^d$ that

$$\Upsilon(s, t, x, w) = x + \mu(s, x)(t - s) + \sigma(s, x)w. \quad (96)$$

Then it holds for all $m, j \in \mathbb{N}_0$, $n \in \{0, 1, \dots, N - 1\}$ that

$$\mathcal{X}_n^{m,j} = \mathcal{X}_n^{m,j} + \mu(t_n, \mathcal{X}_n^{m,j})(t_{n+1} - t_n) + \sigma(t_n, \mathcal{X}_n^{m,j})(W_{t_{n+1}} - W_{t_n}). \quad (97)$$

In the setting of Example 5.4 we consider under suitable further hypotheses for every sufficiently large $m \in \mathbb{N}_0$ the random variable \mathcal{U}^{Θ_m} as an approximation of $u(0, \xi)$ where $u: [0, T] \times \mathbb{R}^d \rightarrow \mathbb{R}^k$ is a suitable solution of the PDE

$$\begin{aligned} \frac{\partial u}{\partial t}(t, x) + \frac{1}{2} \sum_{j=1}^d \left(\frac{\partial^2 u}{\partial x^2} \right)(t, x) (\sigma(t, x) e_j^{(d)}, \sigma(t, x) e_j^{(d)}) + \left(\frac{\partial u}{\partial x} \right)(t, x) \mu(t, x) \\ + f(t, x, u(t, x), \left(\frac{\partial u}{\partial x} \right)(t, x) \sigma(t, x)) = 0 \end{aligned} \quad (98)$$

with $u(T, x) = g(x)$, $e_1^{(d)} = (1, 0, \dots, 0)$, \dots , $e_d^{(d)} = (0, \dots, 0, 1) \in \mathbb{R}^d$ for $t \in [0, T]$, $x = (x_1, \dots, x_d) \in \mathbb{R}^d$ (cf. (PDE) in Section 2 above).

6 Appendix B: PYTHON and MATLAB source codes

6.1 PYTHON source code for an implementation of the deep BSDE solver in the case of the Allen-Cahn PDE (35) in Subsection 4.2

```

1 import time
2 import math
3 import tensorflow as tf
4 import numpy as np
5 from tensorflow.python.training.moving_averages \
6     import assign_moving_average
7 from scipy.stats import multivariate_normal as normal
8 from tensorflow.python.ops import control_flow_ops
9 from tensorflow import random_normal_initializer as norm_init
10 from tensorflow import random_uniform_initializer as unif_init
11 from tensorflow import constant_initializer as const_init
12
13 class SolveAllenCahn(object):
14     """The fully-connected neural network model."""
15     def __init__(self, sess):

```

```

16     self.sess = sess
17     # parameters for the PDE
18     self.d = 100
19     self.T = 0.3
20     # parameters for the algorithm
21     self.n_time = 20
22     self.n_layer = 4
23     self.n_neuron = [self.d, self.d+10, self.d+10, self.d]
24     self.batch_size = 64
25     self.valid_size = 256
26     self.n_maxstep = 4000
27     self.n_displaystep = 100
28     self.learning_rate = 5e-4
29     self.Yini = [0.3, 0.6]
30     # some basic constants and variables
31     self.h = (self.T+0.0)/self.n_time
32     self.sqrth = math.sqrt(self.h)
33     self.t_stamp = np.arange(0, self.n_time)*self.h
34     self._extra_train_ops = []
35
36 def train(self):
37     start_time = time.time()
38     # train operations
39     self.global_step = \
40         tf.get_variable('global_step', [],
41                         initializer=tf.constant_initializer(1),
42                         trainable=False, dtype=tf.int32)
43     trainable_vars = tf.trainable_variables()
44     grads = tf.gradients(self.loss, trainable_vars)
45     optimizer = tf.train.AdamOptimizer(self.learning_rate)
46     apply_op = \
47         optimizer.apply_gradients(zip(grads, trainable_vars),
48                                   global_step=self.global_step)
49     train_ops = [apply_op] + self._extra_train_ops
50     self.train_op = tf.group(*train_ops)
51     self.loss_history = []
52     self.init_history = []
53     # for validation
54     dW_valid, X_valid = self.sample_path(self.valid_size)
55     feed_dict_valid = {self.dW: dW_valid,
56                       self.X: X_valid,
57                       self.is_training: False}
58
59     # initialization
60     step = 1
61     self.sess.run(tf.global_variables_initializer())
62     temp_loss = self.sess.run(self.loss,
63                               feed_dict=feed_dict_valid)
64     temp_init = self.Y0.eval()[0]
65     self.loss_history.append(temp_loss)

```

```

65     self.init_history.append(temp_init)
66     print "step: %5u, loss: %.4e, " % \
67           (0, temp_loss) + \
68           "Y0: %.4e, runtime: %4u" % \
69           (temp_init, time.time()-start_time+self.t_bd)
70     # begin sgd iteration
71     for _ in range(self.n_maxstep+1):
72         step = self.sess.run(self.global_step)
73         dW_train, X_train = self.sample_path(self.batch_size)
74         self.sess.run(self.train_op,
75                       feed_dict={self.dW: dW_train,
76                                   self.X: X_train,
77                                   self.is_training: True})
78         if step % self.n_displaystep == 0:
79             temp_loss = self.sess.run(self.loss,
80                                       feed_dict=feed_dict_valid)
81             temp_init = self.Y0.eval()[0]
82             self.loss_history.append(temp_loss)
83             self.init_history.append(temp_init)
84             print "step: %5u, loss: %.4e, " % \
85                   (step, temp_loss) + \
86                   "Y0: %.4e, runtime: %4u" % \
87                   (temp_init, time.time()-start_time+self.t_bd)
88             step += 1
89         end_time = time.time()
90         print "running time: %.3f s" % \
91               (end_time-start_time+self.t_bd)
92
93     def build(self):
94         start_time = time.time()
95         # build the whole network by stacking subnetworks
96         self.dW = tf.placeholder(tf.float64,
97                                  [None, self.d, self.n_time],
98                                  name='dW')
99         self.X = tf.placeholder(tf.float64,
100                                [None, self.d, self.n_time+1],
101                                name='X')
102         self.is_training = tf.placeholder(tf.bool)
103         self.Y0 = tf.Variable(tf.random_uniform([1],
104                                                minval=self.Yini[0],
105                                                maxval=self.Yini[1],
106                                                dtype=tf.float64));
107         self.Z0 = tf.Variable(tf.random_uniform([1, self.d],
108                                                minval=-.1,
109                                                maxval=.1,
110                                                dtype=tf.float64))
111         self.allones = \
112             tf.ones(shape=tf.pack([tf.shape(self.dW)[0], 1]),
113                    dtype=tf.float64)

```

```

114     Y = self.allones * self.Y0
115     Z = tf.matmul(self.allones, self.Z0)
116     with tf.variable_scope('forward'):
117         for t in xrange(0, self.n_time-1):
118             Y = Y - self.f_tf(self.t_stamp[t],
119                               self.X[:, :, t], Y, Z)*self.h
120             Y = Y + tf.reduce_sum(Z*self.dW[:, :, t], 1,
121                                   keep_dims=True)
122             Z = self._one_time_net(self.X[:, :, t+1],
123                                   str(t+1))/self.d
124         # terminal time
125         Y = Y - self.f_tf(self.t_stamp[self.n_time-1],
126                           self.X[:, :, self.n_time-1],
127                           Y, Z)*self.h
128         Y = Y + tf.reduce_sum(Z*self.dW[:, :, self.n_time-1], 1,
129                               keep_dims=True)
130         term_delta = Y - self.g_tf(self.T,
131                                   self.X[:, :, self.n_time])
132         self.clipped_delta = \
133             tf.clip_by_value(term_delta, -50.0, 50.0)
134         self.loss = tf.reduce_mean(self.clipped_delta**2)
135     self.t_bd = time.time()-start_time
136
137     def sample_path(self, n_sample):
138         dW_sample = np.zeros([n_sample, self.d, self.n_time])
139         X_sample = np.zeros([n_sample, self.d, self.n_time+1])
140         for i in xrange(self.n_time):
141             dW_sample[:, :, i] = \
142                 np.reshape(normal.rvs(mean=np.zeros(self.d),
143                                       cov=1,
144                                       size=n_sample)*self.sqrth,
145                             (n_sample, self.d))
146             X_sample[:, :, i+1] = X_sample[:, :, i] + \
147                 np.sqrt(2) * dW_sample[:, :, i]
148         return dW_sample, X_sample
149
150     def f_tf(self, t, X, Y, Z):
151         # nonlinear term
152         return Y-tf.pow(Y, 3)
153
154     def g_tf(self, t, X):
155         # terminal conditions
156         return 0.5/(1 + 0.2*tf.reduce_sum(X**2, 1, keep_dims=True))
157
158     def _one_time_net(self, x, name):
159         with tf.variable_scope(name):
160             x_norm = self._batch_norm(x, name='layer0_normal')
161             layer1 = self._one_layer(x_norm, self.n_neuron[1],
162                                     name='layer1')

```



```

163         layer2 = self._one_layer(layer1, self.n_neuron[2],
164                                 name='layer2')
165         z = self._one_layer(layer2, self.n_neuron[3],
166                             activation_fn=None, name='final')
167     return z
168
169     def _one_layer(self, input_, out_sz,
170                  activation_fn=tf.nn.relu,
171                  std=5.0, name='linear'):
172     with tf.variable_scope(name):
173         shape = input_.get_shape().as_list()
174         w = tf.get_variable('Matrix',
175                             [shape[1], out_sz], tf.float64,
176                             norm_init(stddev= \
177                                     std/np.sqrt(shape[1]+out_sz)))
178         hidden = tf.matmul(input_, w)
179         hidden_bn = self._batch_norm(hidden, name='normal')
180     if activation_fn != None:
181         return activation_fn(hidden_bn)
182     else:
183         return hidden_bn
184
185     def _batch_norm(self, x, name):
186     """Batch normalization"""
187     with tf.variable_scope(name):
188         params_shape = [x.get_shape()[-1]]
189         beta = tf.get_variable('beta', params_shape,
190                                tf.float64,
191                                norm_init(0.0, stddev=0.1,
192                                           dtype=tf.float64))
193         gamma = tf.get_variable('gamma', params_shape,
194                                 tf.float64,
195                                 unif_init(0.1, 0.5,
196                                           dtype=tf.float64))
197         mv_mean = tf.get_variable('moving_mean',
198                                   params_shape,
199                                   tf.float64,
200                                   const_init(0.0, tf.float64),
201                                   trainable=False)
202         mv_var = tf.get_variable('moving_variance',
203                                  params_shape,
204                                  tf.float64,
205                                  const_init(1.0, tf.float64),
206                                  trainable=False)
207         # These ops will only be performed when training
208         mean, variance = tf.nn.moments(x, [0], name='moments')
209         self._extra_train_ops.append(\
210             assign_moving_average(mv_mean, mean, 0.99))
211         self._extra_train_ops.append(\

```

```

212         assign_moving_average(mv_var, variance, 0.99))
213     mean, variance = \
214         control_flow_ops.cond(self.is_training,
215                               lambda: (mean, variance),
216                               lambda: (mv_mean, mv_var))
217     y = tf.nn.batch_normalization(x, mean, variance,
218                                  beta, gamma, 1e-6)
219     y.set_shape(x.get_shape())
220     return y
221
222 def main():
223     tf.reset_default_graph()
224     with tf.Session() as sess:
225         tf.set_random_seed(1)
226         print "Begin to solve Allen-Cahn equation"
227         model = SolveAllenCahn(sess)
228         model.build()
229         model.train()
230         output = np.zeros((len(model.init_history), 3))
231         output[:, 0] = np.arange(len(model.init_history)) \
232             * model.n_displaystep
233         output[:, 1] = model.loss_history
234         output[:, 2] = model.init_history
235         np.savetxt("./AllenCahn_d100.csv",
236                   output,
237                   fmt=['%d', '%.5e', '%.5e'],
238                   delimiter=",",
239                   header="step, loss function, " + \
240                       "target value, runtime",
241                   comments='')
242
243 if __name__ == '__main__':
244     np.random.seed(1)
245     main()

```

MATLAB code 1: A PYTHON code for the deep BSDE solver in Subsection 3.2 in the case of the PDE (35).

6.2 MATLAB source code for the Branching diffusion method used in Subsection 4.2

```

1 function Branching_Matlab()
2 % Parameters for the model
3 T = 0.3; t0 = 0; x0 = 0; d = 100; m = d;
4 mu = zeros(d,1); sigma = eye(d)*sqrt(2);
5 a = [0 2 0 -1]';

```

```

6   g = @(x) 1./(1+0.2*norm(x)^2)*1/2;
7
8   % Parameters for the algorithm
9   rng('default'); M = 10^7; beta = 1; p = [0 0.5 0 0.5]';
10
11  % Branching method
12  tic;
13  [mn,sd] = MC_BM( mu, sigma, beta, p, a, t0, x0, T, g, M );
14  runtime = toc;
15
16  % Output
17  disp(['Terminal condition: u(T,x0) = ' num2str(g(x0)) '']);
18  disp(['Branching method: u(0,x0) ~ ' num2str(mn) '']);
19  disp(['Estimated standard deviation: ' num2str(sd) '']);
20  disp(['Estimated L2-appr. error = ' num2str(sd/sqrt(M)) '']);
21  disp(['Elapsed runtime = ' num2str(runtime) '']);
22  end
23
24  function [mn,sd] = MC_BM(mu, sigma, beta, p, a, t0, x0, T, g, M)
25      mn = 0; sd = 0;
26      for m=1:M
27          result = BM_Eval(mu, sigma, beta, p, a, t0, x0, T, g);
28          mn = mn + result;
29          sd = sd + result^2;
30      end
31      mn = mn/M; sd = sqrt( (sd - mn^2/M)/M );
32  end
33
34  function result = BM_Eval(mu, sigma, beta, p, a, t0, x0, T, g)
35      bp = BP(mu, sigma, beta, p, t0, x0, T);
36      result = 1;
37      for k=1:size(bp{1},2)
38          result = result * g( bp{1}(:,k) );
39      end
40      if norm(a-p) > 0
41          for k=1:length(a)
42              if p(k) > 0
43                  result = result * ( a(k)/p(k) )^( bp{2}(k) );
44              elseif a(k) ~= 0
45                  error('a(k) zero but p(k) non-zero');
46              end
47          end
48      end
49  end
50
51  function bp = BP(mu, sigma, beta, p, t0, x0, T)
52      bp = cell(2,1);
53      bp{2} = p*0;
54      tau = exprnd(1/beta);

```

```

55 new_t0 = min( tau + t0, T );
56 delta_t = new_t0 - t0;
57 m = size(sigma,2);
58 new_x0 = x0 + mu*delta_t + sigma*sqrt(delta_t)*randn(m,1);
59 if tau >= T - t0
60     bp{1} = new_x0;
61 else
62     [tmp,nonlinearity] = max(mnrnd(1,p));
63     bp{2}(nonlinearity) = bp{2}(nonlinearity) + 1;
64     for k=1:nonlinearity-1
65         tmp = BP(mu, sigma, beta, p, new_t0, new_x0, T);
66         bp{1} = [ bp{1} tmp{1} ];
67         bp{2} = bp{2} + tmp{2};
68     end
69 end
70 end

```

MATLAB code 2: A MATLAB code for the Branching diffusion method in the case of the PDE (35) based on $M = 10^7$ independent realizations.

6.3 MATLAB source code for the classical Monte Carlo method used in Subsection 4.3

```

1 function MonteCarlo_Matlab()
2     rng('default');
3
4     % Parameters for the model
5     d = 100;
6     g = @(x) log( (1+norm(x)^2)/2 );
7     T = 1;
8     M = 10^7;
9     t = 0;
10
11    % Classical Monte Carlo
12    tic;
13    MC = 0;
14    for m=1:M
15        dW = randn(1,d)*sqrt(T-t);
16        MC = MC + exp( - g( dW * sqrt(2) ) );
17    end
18    MC = -log(MC/M);
19    runtime = toc;
20
21    % Output
22    disp(['Solution: u(T,0) = ' num2str(g(0)) ',';']);
23    disp(['Solution: u(0,0) = ' num2str(MC) ',';']);

```

```

24     disp(['Time = ' num2str(runtime) '']);
25 end

```

MATLAB code 3: A MATLAB code for a Monte Carlo method related to the PDE (36) based on $M = 10^7$ independent realizations.

Acknowledgements

Christian Beck and Sebastian Becker are gratefully acknowledged for useful suggestions regarding the implementation of the deep BSDE solver. This project has been partially supported through the Major Program of NNSFC under grant 91130005, the research grant ONR N00014-13-1-0338, and the research grant DOE DE-SC0009248.

References

- [1] BELLMAN, R. *Dynamic programming*. Princeton Landmarks in Mathematics. Princeton University Press, Princeton, NJ, 2010. Reprint of the 1957 edition, With a new introduction by Stuart Dreyfus.
- [2] BENDER, C., AND DENK, R. A forward scheme for backward SDEs. *Stochastic Processes and their Applications* 117, 12 (2007), 1793–1812.
- [3] BENDER, C., SCHWEIZER, N., AND ZHUO, J. A primal-dual algorithm for BSDEs. *arXiv:1310.3694* (2014), 36 pages.
- [4] BERGMAN, Y. Z. Option pricing with differential interest rates. *Review of Financial Studies* 8, 2 (1995), 475–500.
- [5] BRIAND, P., AND LABART, C. Simulation of BSDEs by Wiener chaos expansion. *Ann. Appl. Probab.* 24, 3 (06 2014), 1129–1171.
- [6] CHASSAGNEUX, J.-F. Linear multistep schemes for BSDEs. *SIAM J. Numer. Anal.* 52, 6 (2014), 2815–2836.
- [7] CHASSAGNEUX, J.-F., AND RICHOU, A. Numerical simulation of quadratic BSDEs. *Ann. Appl. Probab.* 26, 1 (2016), 262–304.
- [8] CRISAN, D., AND MANOLARAKIS, K. Solving backward stochastic differential equations using the cubature method: Application to nonlinear pricing. *SIAM Journal on Financial Mathematics* 3, 1 (2012), 534–571.

- [9] DARBON, J., AND OSHER, S. Algorithms for overcoming the curse of dimensionality for certain Hamilton-Jacobi equations arising in control theory and elsewhere. *Res. Math. Sci.* 3 (2016), Paper No. 19, 26.
- [10] DEBNATH, L. *Nonlinear partial differential equations for scientists and engineers*, third ed. Birkhäuser/Springer, New York, 2012.
- [11] E, W., HUTZENTHALER, M., JENTZEN, A., AND KRUSE, T. On full history recursive multilevel Picard approximations and numerical approximations for high-dimensional nonlinear parabolic partial differential equations and high-dimensional nonlinear backward stochastic differential equations. *arXiv:1607.03295* (2017), 46 pages.
- [12] GOBET, E., LEMOR, J.-P., AND WARIN, X. A regression-based Monte Carlo method to solve backward stochastic differential equations. *Ann. Appl. Probab.* 15, 3 (2005), 2172–2202.
- [13] GOBET, E., AND TURKEDJIEV, P. Linear regression MDP scheme for discrete backward stochastic differential equations under general conditions. *Math. Comp.* 85, 299 (2016), 1359–1391.
- [14] GOBET, E., AND TURKEDJIEV, P. Adaptive importance sampling in least-squares Monte Carlo algorithms for backward stochastic differential equations. *Stochastic Process. Appl.* 127, 4 (2017), 1171–1203.
- [15] GOODFELLOW, I., BENGIO, Y., AND COURVILLE, A. *Deep Learning*. MIT Press, 2016. <http://www.deeplearningbook.org>.
- [16] HAN, J., AND E, W. Deep Learning Approximation for Stochastic Control Problems. *arXiv:1611.07422* (2016), 9 pages.
- [17] HENRY-LABORDÈRE, P. Counterparty risk valuation: a marked branching diffusion approach. *arXiv:1203.2369* (2012), 17 pages.
- [18] HENRY-LABORDÈRE, P., OUDJANE, N., TAN, X., TOUZI, N., AND WARIN, X. Branching diffusion representation of semilinear PDEs and Monte Carlo approximation. *arXiv:1603.01727* (2016), 30 pages.
- [19] HENRY-LABORDÈRE, P., TAN, X., AND TOUZI, N. A numerical algorithm for a class of BSDEs via the branching process. *Stochastic Process. Appl.* 124, 2 (2014), 1112–1140.
- [20] HINTON, G. E., DENG, L., YU, D., DAHL, G., MOHAMED, A., JAITLY, N., SENIOR, A., VANHOUCHE, V., NGUYEN, P., SAINATH, T., AND KINGSBURY, B.

- Deep neural networks for acoustic modeling in speech recognition. *Signal Processing Magazine* 29 (2012), 82–97.
- [21] IOFFE, S., AND SZEGEDY, C. *Batch normalization: accelerating deep network training by reducing internal covariate shift*. Proceedings of The 32nd International Conference on Machine Learning (ICML), June 2015.
- [22] KINGMA, D., AND BA, J. *Adam: a method for stochastic optimization*. Proceedings of the International Conference on Learning Representations (ICLR), May 2015.
- [23] KRIZHEVSKY, A., SUTSKEVER, I., AND HINTON, G. E. Imagenet classification with deep convolutional neural networks. *Advances in Neural Information Processing Systems* 25 (2012), 1097–1105.
- [24] LECUN, Y., BENGIO, Y., AND HINTON, G. Deep learning. *Nature* 521 (2015), 436–444.
- [25] PARDOUX, É., AND PENG, S. Backward stochastic differential equations and quasilinear parabolic partial differential equations. In *Stochastic partial differential equations and their applications (Charlotte, NC, 1991)*, vol. 176 of *Lecture Notes in Control and Inform. Sci.* Springer, Berlin, 1992, pp. 200–217.
- [26] PARDOUX, É., AND PENG, S. G. Adapted solution of a backward stochastic differential equation. *Systems Control Lett.* 14, 1 (1990), 55–61.
- [27] PARDOUX, E., AND TANG, S. Forward-backward stochastic differential equations and quasilinear parabolic PDEs. *Probab. Theory Related Fields* 114, 2 (1999), 123–150.
- [28] PENG, S. G. Probabilistic interpretation for systems of quasilinear parabolic partial differential equations. *Stochastics Stochastics Rep.* 37, 1-2 (1991), 61–74.